CODEN:LUTEDX/(TEIE-5412)/1-72(2018)

Industrial Electrical Engineering and Automation

Energy Harvesting with Solar Cells for Wireless Alarm Nodes

Tobias Olofsson

Division of Industrial Electrical Engineering and Automation
Faculty of Engineering, Lund University

Energy Harvesting with Solar Cells for Wireless Alarm Nodes

Tobias Olofsson

Division of Industrial Electrical Engineering and Automation
Faculty of Engineering
Lund University

2018

Supervisor: Gunnar Lindstedt

Assisting supervisor: Jonas Johannesson

Examiner: Johan Björnstedt

Abstract

The power consumption of electronic devices is decreasing at the same time as the performance of solar cells is increasing. Solar cells based on new technologies with lower costs are becoming commercially available, creating new opportunities for use in small electronic products. The concept of capturing ambient energy, such as light, and using it to power small electronic devices is known as energy harvesting. Modern home alarm systems consist of wireless nodes with different power requirements and which are placed in different locations with different light conditions. One common wireless alarm node is the magnet contact, which is often placed on windows or on doors. The window location is very interesting as it provides good conditions for harvesting energy with solar cells.

This thesis investigates the three subsystems which are typically part of an energy harvesting system; solar cells, energy storage and power electronics. Different options for the three subsystems are considered and compared keeping the application in mind, harvesting energy for wireless alarm nodes. The literature studies are complemented by investigations of the market to get a rough estimate of the cost of each system. Measurements on three types of solar cells are made both in a home environment and in a lab environment to estimate the amount of energy that can be harvested in natural and artificial light. Finally, the concept of harvesting energy with solar cells for wireless alarm nodes is demonstrated by building a prototype for the magnet contact alarm node.

The result from the investigation shows that there are many ways to design an energy harvesting system, and that the solution very much depends on the maximum acceptable cost. The functionality of the prototype is demonstrated, although further tests are required to assess the year-round behavior.

Sammanfattning

Energiförbrukningen i elektronikprodukter minskar samtidigt som prestandan för solceller hela tiden ökar. Nya solcellstyper med lägre priser skapar nya möjligheter för använding även i små elektronikprodukter. Att samla energi från omgivningen, t.ex. från ljuset i ett rum, och använda det för att driva små elektronikprodukter kallas i ett vidare begrepp för ”energy harvesting” (SV: energiskördning). Moderna larmsystem består av trådlösa larmnoder, med olika energiförbrukning, som installeras på olika platser med olika ljusförhållanden. En vanligt förekommande trådlös larmnod är magnetkontakten, vilken ofta installeras i fönster och på dörrar. Fönsterläget är särskillt intressant eftersom där finns goda ljusförhållanden, vilket ökar potentialen i användning av solceller.

Denna avhandling behandlar de tre delsystemen som typiskt ingår i ett ”energy harvesting”-system; solceller, batterier och kraftelektronik. Olika alternativ för de tre delsystemen övervägs och jämförs, med applikation för trådlösa larmnoder i åtanke. Litteraturstudier kompletteras med undersökningar av marknaden för att estimera vad de olika systemen kan kosta. Mätningar på tre typer av solceller görs både i hemmiljö och i labbmiljö för att estimera hur mycket energi som kan skördas i naturligt och artificiellt ljus. Slutligen demonstreras konceptet av att skörda energi till larmnoder genom att bygga en prototyp för magnetkontakten.

Resultatet från undersökningen visar att det går att bygga ett ”energy-harvesting”-system på många sätt och att valet av lösning starkt beror på hur mycket lösningen får kosta. Funktionaliteten av prototypen demonstreras, men fortsatta tester krävs för att avgöra hur den beter sig året runt.

Abbreviations

AM1.5 = air mass 1.5

AREF = analog reference

a-Si = amorphous silicon

CAD = computer-aided design

CCCV = constant current constant voltage

CdTe = cadmium telluride

CFL = compact fluorescent lamp

CIGS = copper indium gallium selenide

c-Si = crystalline silicon

DC = direct current

DoD = depth of discharge

DSSC = dye-sensitized solar cell

EDLC = electrochemical double-layer capacitor

ESR = equivalent series resistance

F.OCV = fractional open-circuit voltage

GaAs = gallium arsenide

IC = integrated circuit

IR = infrared

I-V = current-voltage

ku = 1000 units

LED = light-emitting diode

Li-ion = lithium-ion

low-E = low emissivity

MPP = maximum power point

MPPT = maximum power point tracking

NiMH = nickel metal hydride

NREL = National Renewable Energy Laboratory

OCV = open-circuit voltage

OSC = organic solar cell

PC = personal computer

PCB = printed circuit board

PSC = perovskite solar cell

QDSC = quantum dot solar cell

SCC = short-circuit current

SMHI = Swedish Meteorological and Hydrological Institute

STC = standard test conditions

USB = universal serial bus

UV = ultraviolet

Table of Contents

1 INTRODUCTION

1.1 BACKGROUND

Modern home alarm systems consist of wireless alarm nodes with different functionality and power demands installed at different locations throughout the house. Most of the alarm nodes are powered by batteries while the alarm panel of the system is often powered with the help of a wall adapter. With the decreasing power consumption of electronics and the decreasing price and increasing capabilities of solar cells, it is interesting to investigate what energy harvesting can do for wireless alarm nodes and if it can reduce the need for batteries.

1.2 PROBLEM FORMULATION

The main goal of this thesis is to investigate the possibilities of using solar cells to power wireless alarm nodes. The concept is demonstrated by building a prototype of an alarm node powered by solar cells.

The following questions are treated:

1. **Available energy:** How much energy can be harvested at locations typical for the wireless alarm nodes?
2. **Solar cells:** How does different solar cells compare with respect to relevant parameters such as efficiency and price?
3. **Power electronics:** What power electronics is required to make the energy harvesting solution efficient and what are the consequences in cost?
4. **Energy storage:** Which types of storage can be used for storing the harvested energy and how do they compare?
5. **Prolonged battery life:** How can energy harvesting with solar cells be used to prolong the battery life of primary batteries (non-rechargeable batteries)?

1.3 LIMITATIONS

The investigation of available energy is focused around the typical locations for the magnet contact alarm node and is therefore limited to windows and doors (a “magnet contact” is an alarm sensor that is normally put on windows and doors). The measurements are limited to the geographical location of southern Sweden.

The work is focused on the electrical aspects of using solar cells for energy harvesting, and less focused on topics such as mechanical integration and design.

The prototype energy harvesting system designed in this thesis includes the use of primary batteries (non-rechargeable batteries) but does not consider the different types of primary batteries that are available.

1.4 REPORT OUTLINE

Chapter 1 describes the subject of the thesis, defines the questions that should be answered and the limitations of the work.

Chapter 2 describes the methodology used to reach the goal of the thesis.

Chapters 3-5 treat the three subsystems of an energy harvesting solution; solar cells, energy storage and power electronics. These chapters are based on information collected through literature and from market investigations.

Chapter 6 includes a description and the results from measurements made on solar cells in both a home environment and in a lab environment.

Chapter 7 describes the design process and evaluation of a prototype of a solar cell driven magnet contact alarm node.

Chapter 8 discusses the information that was collected throughout the thesis and how it applies to wireless alarm nodes.

Chapter 9 concludes the report with conclusions and suggestions for future work.

2 METHOD

The first question regarding the amount of energy that is available in a home is treated by first reading literature to understand how the output power of solar cells depend on the incident light and then studying different light sources and their spectral content. Measurements are then done on different solar cells in light from different sources to understand how they contribute to the total amount of energy that can be harvested. The energy that can be harvested from natural light is investigated in a home environment at two locations which are typical for the magnet contact alarm node. A lab environment is used to find out how much power the solar cells can harvest in different types of artificial light.

The questions which concern the three subsystems of an energy harvesting system; solar cells, energy storage and power electronics (questions 2-4) are treated by collecting information from literature and from market investigations. The options for solar cells, energy storage and power electronics are then discussed with the application in mind to deduce if they are viable, the pros and cons of the different alternatives and when feasible discuss when to use one over the other.

Question 5 regarding how energy harvesting can prolong the battery life of primary batteries is treated by showing how an electrical solution for harvesting energy can automatically switch to using backup batteries when the rechargeable storage is depleted. It is discussed how this solution can be used to achieve the goal of prolonging battery life.

When the five main questions have been treated, a prototype is built around the magnet contact alarm node to test the concept and to learn more about the challenges of implementing an energy harvesting system.

3 SOLAR CELLS

This chapter introduces the basics of solar cells; how they operate and how different solar cells can be compared. Common light sources and the spectrums of their emitted light are explained next. Finally, this chapter presents different types of solar cells and their respective properties.

3.1 BASIC OPERATION

Solar cells produce a voltage and a current when they are exposed to incident light. They are both used in large scale power generation and in smaller products to reduce the need for batteries e.g. pocket calculators.

Traditional crystalline silicon based solar cells consist of a p-n junction which is formed when two oppositely doped semiconductor materials are brought together. When light with sufficient energy hits the semiconductor material, electrons are excited forming hole-electron pairs. The hole-electron pairs are separated with the help of the internal electric field which forms naturally at the p-n junction. Depending on which side the pair was formed on, the electron or the hole then travels across the p-n junction while the other travels through an external load connected to the solar cell. When the electron and hole finally meet again at the other side, they recombine, and the electron returns to a lower energy band. [1] [2]

Since the p-n junction effectively separates the hole-electron pairs into electrons on one side and holes on the other side, a difference in electrical charge exists on the two sides. This difference in electrical charge creates a difference in potential between the two sides. This is known as the photovoltaic effect and is a fundamental part of how solar cells work. When the load connected to the solar cell is of low electrical resistance, the charges can easily leave the solar cell and travel through the load. The charge buildup at the electrodes is then small and the voltage across the solar cell is therefore also small. When the resistance of the load is large, fewer charges can leave the cell and the voltage across the solar cell is therefore greater than for a low resistance load. [3]

For this reason, the magnitude of the current and the magnitude of the voltage produced by a solar cell is always a compromise. An I-V curve shows how the voltage and current of a solar cell are related. The typical form of an I-V curve is shown in Figure 1.

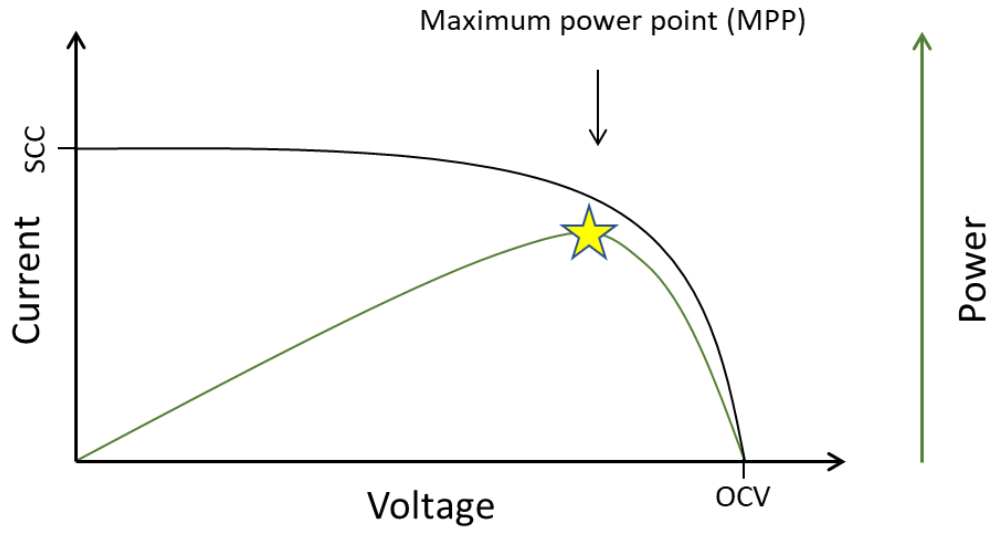

Figure 1: Shows a typical I-V curve of a solar cell (black) along with the power curve (green).

The power curve that is seen in Figure 1 can be obtained by multiplying the voltage by the current at each point. As can be seen in the graph the power curve has a maximum point at a specific voltage level. This operating point which results in maximum power is called the maximum power point (MPP). To work at maximum efficiency the solar cells should stay at the MPP, which can be achieved by matching the load impedance to the impedance of the MPP, a process which is further explained in chapter 5.1.

As shown in Figure 1, at the point on the I-V curve where the current is zero, the voltage is called the open-circuit voltage (OCV). At the point at which the voltage is zero the current is called the short-circuit current (SCC). [3]

A common way to compare solar cells is to compare their efficiency. The efficiency is a measurement of how much of the power P_{in} of the incident light that can be extracted when working at the MPP (P_{max}), as defined by equation (1). [4]

$$\eta = \frac{P_{max}}{P_{in}} \tag{1}$$

The efficiency of a solar cell is usually measured under standard test conditions (STC), which assume a temperature of 25° C, an irradiance of 1000 W/m^2 and the AM1.5 spectrum (air mass 1.5). AM1.5 implies that the incident light has a spectrum which is equivalent to the spectrum of sunlight when the light has travelled a certain distance in the Earth's atmosphere and thus lost a certain amount of the intensity of each wavelength due to atmospheric absorption and other effects. AM1 implies that the light has travelled a distance in the atmosphere which is equivalent to when the sun is directly overhead, while AM1.5 implies that the light has travelled a distance that is 1.5 times as long corresponding to a zenith angle of 48.2° for the Sun (zenith angle is the angle between a line going directly upwards and the Sun). [4] [5] [6]

The short-circuit current increases linearly with the intensity of the light that is incident on the solar cell. The open-circuit voltage also increases with the light intensity, but with a much slower rate. An illustration of how the I-V curve changes with the light intensity is shown in Figure 2. [7]

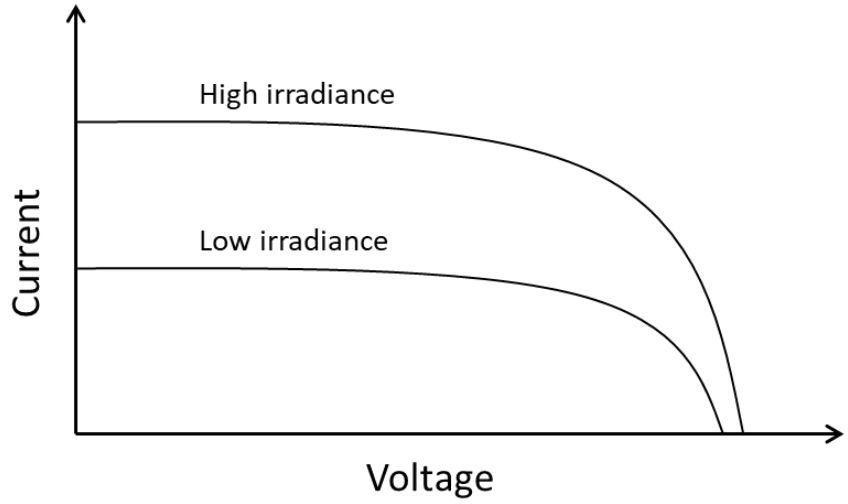

Figure 2: Shows how the I-V curve of a solar cell changes with changing light intensity.

The current produced by a solar cell is not only dependent on the light intensity, but also on the wavelengths of the incident light. Different wavelengths contribute in different proportions to the

current that is produced. One way to state the dependence of wavelength for a particular solar cell is through the quantum efficiency. The quantum efficiency is the ratio between the hole-electron pairs which are successfully separated at the p-n junction to the number of incident photons of a specific wavelength. [8]

The wavelengths for which the quantum efficiency is high varies between different types of solar cells. When choosing solar cell, the spectrum of the light that it will placed in should therefore be considered and the quantum efficiency window should preferably match it well.

Traditional semiconductor based solar cells have a temperature dependence which decreases the OCV and increases the SCC when the temperature of the solar cell increases. The decrease of the OCV is the dominating effect resulting in a lower power output as the temperature increases. Temperature dependence of a solar cell is often stated as the temperature coefficient for both voltage and current in units of [% / °C] which can be used to calculate how the voltage and current deviates from the rated values. [9]

The current from the solar cell is proportional to the area of the solar cell. To increase the current and in turn the power, the area of the cell can be increased or many solar cells can be put in parallel. To increase the voltage, which also increases the power, many cells can be put in series. When many solar cells are connected together the whole package is referred to as a solar cell module.

3.2 LIGHT

This chapter introduces the most common sources of light and discusses how the output power of a particular solar cell in a particular light condition can be found.

3.2.1 Light sources

A fundamental way to classify a light source is through its spectral content. Different sources of light emit light with different wavelengths. The Sun emits light with a wide range of wavelengths while the light from a LED lamp is mostly visible light, which includes wavelengths in the 400-700 nm range.

3.2.1.1 The Sun

The spectrum of the solar radiation is close to the theoretical spectrum of a blackbody at 5800 K [10], for which the spectral radiance is shown in Figure 3. The spectrum of the sunlight experienced on the Earth is however not exactly that of an ideal blackbody. Different gases in the Earth's atmosphere absorb light of specific wavelengths. These gases include water vapor, carbon dioxide and ozone [11]. This results in a spectrum at the Earth which has lower levels of irradiance for the same wavelengths.

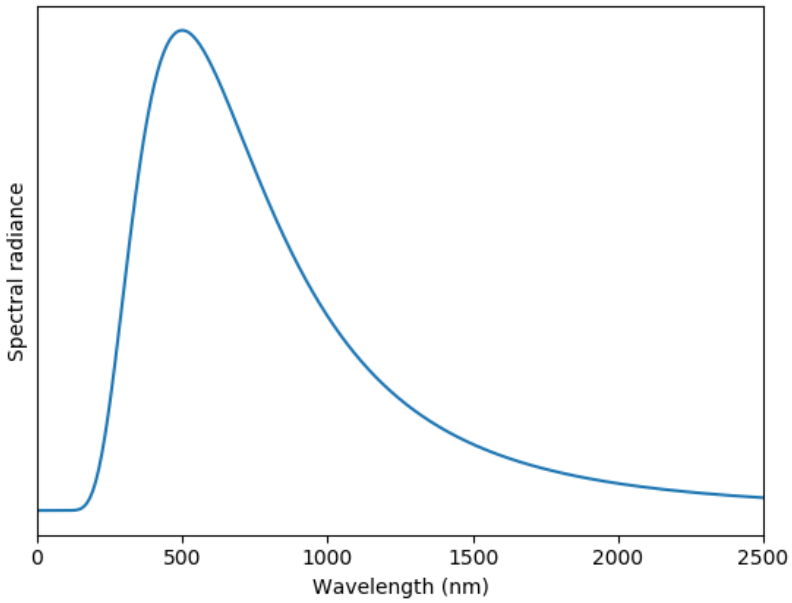

Figure 3: Spectral radiance for a blackbody at 5800 K (representing the Sun).

When sunlight shines through the windows of a building it also loses some of its energy. Glass windows typically block UV radiation [12]. Furthermore, to reduce the heat loss through radiation from a building some windows have a coating which reflects IR light (infrared radiation, IR, includes wavelengths from 700 nm to 1 mm). These windows are known as low-emissivity windows (low-E windows).

3.2.1.2 Artificial light sources

Three common artificial light sources and the wavelengths of the light they emit are described in this chapter, including LED lamps, fluorescent lamps and halogen lamps.

LED lamps are today very popular for all kinds of applications due to their low power consumption and long lifetime. By themselves LED lamps have a very narrow range of emitted wavelengths, but together with a phosphor they can be made to emit white light which includes all the visible colors. The wavelengths of the emitted light are mostly inside the range of visible light (400-700 nm).

A fluorescent lamp has a tube which contains a gas of argon or mercury which is excited to emit UV-light. The gas is excited when a high voltage is applied at the ends of the tube, which then forces a current through the gas. The inside of the tube is coated with a phosphor which emits light in the visible range when hit by the UV-light (400-700 nm). [13]

In an incandescent lamp a thin wire is heated to a high temperature so that it emits radiation in the visible spectrum [13]. The spectrum of the emitted light is close to that of a blackbody with the same temperature as the wire (usually 2700 K). This means that a big part of the emitted energy consists of longer wavelengths which are not visible to the human eye, as shown in Figure 4. Since a lot of power to heat the wire is radiated as light outside of the visible spectrum, this lamp has a low efficiency. This has led to regulations in the European Union to the point where these types of lamps are not used so much anymore [13], and they may therefore be less relevant to investigate for the purpose of energy harvesting for alarm systems in personal homes. A more efficient version of the incandescent lamp is the halogen lamp.

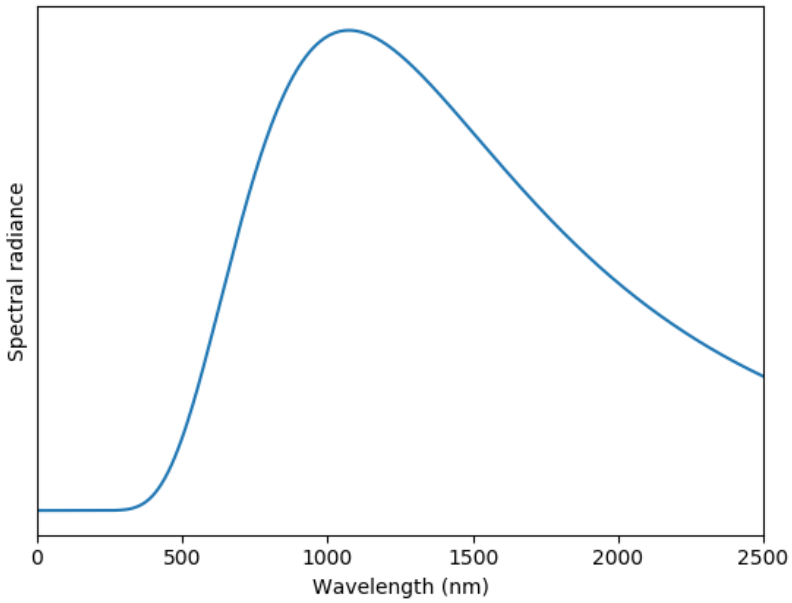

Figure 4: Spectral radiance for a blackbody at 2700 K (representing an incandescent lamp).

3.2.2 Predicting solar cell output power by measuring light

A common way of quantifying light is by expressing the illuminance in units of lux, for which a number can be easily obtained with the help of a lux meter, which exist as portable handheld devices.

The illuminance is a quantity which expresses the luminous flux ϕ_v per unit area A, as shown in equation 2-3. The luminous flux ϕ_v is formed by weighting the power of the different wavelengths in the spectrum of the incident light by the luminosity function. The result is a number which is representative for the perceived brightness of the human eye, thus the luminosity function only takes into account the wavelengths in the visible range (approximately 400-700 nm). Because different light conditions can produce the same illuminance even though they have different spectral content the illuminance is not a good measurement for predicting the output power of solar cells, as the output power of solar cells is highly dependent on the spectral content. [14]

$$E_v = \frac{\phi_v}{A} = [lux] \tag{2}$$

$$\phi_v = \text{"spectral content weighted by the luminosity function"} = [lm] \tag{3}$$

A more sophisticated approach for quantifying light and predicting the output power of solar cells is to use a spectrometer to measure the intensity of each wavelength in the incident light. However, spectrometers are expensive, usually not very portable and would produce large data volumes if they would be set up to log how the light changes over time. When the light spectrum has been captured it is also required that the spectral response of the solar cell is available, that is the relation used to translate the spectrum of the incident light to the current produced by the solar cell. [14]

A more practical way to find out how much power a solar cell can produce is to perform measurements directly on the solar cells in the light conditions that are of interest. It is then required to have an analog circuit which varies the load experienced by the solar cell such that the I-V curve can be captured to find the maximum power. This is the approach that is used in this thesis and specifically used for the measurements that are presented in chapter 6.

3.3 SOLAR CELL TECHNOLOGIES

New types of solar cells are actively being explored, although the majority of solar cells produced today are based on crystalline silicon [15]. The different solar cell technologies are often divided into three generations, as can be seen in Table 1 .

The solar cells belonging to the first generation are made from wafers which are slices of semiconductor material with crystalline structures. Solar cells in the second generation are called thin films because they can be made much thinner requiring less material and thereby reducing costs. The third generation of solar cells includes technologies based on new concepts exploring new materials and techniques which can possibly overcome the efficiency limits of the previous technologies. These solar cells have typically not had their commercial breakthrough yet, although some products have recently become available. [16] [17]

Table 1: Notable solar cell technologies divided into three generations [18].

Generation 1	**Generation 2**	**Generation 3**
Crystalline silicon (c-Si)	Amorphous silicon (a-Si)	Multi-junction
	Cadmium telluride (CdTe)	Organic (OSC)
	Copper indium gallium selenide (CIGS)	Dye-sensitized (DSSC)
	Gallium arsenide (GaAs)	Perovskite (PSC)
		Quantum dot (QDSC)

The following chapters describes crystalline silicon solar cells which currently dominate the market, along with three technologies with lower costs which is important for electronic products such as alarm nodes. These technologies include amorphous silicon which is well established and belong to the second generation thin film solar cells, and two technologies belonging to the third generation; organic and dye-sensitized solar cells, which are both available as products on the market today. The remaining technologies shown in Table 1 are briefly mentioned.

Multi-junction solar cells involve the use of multiple p-n junctions to create solar cells with very high efficiency. Each p-n junction can be of made of different materials specialized at capturing different parts of the light spectrum such that a high total efficiency can be achieved. These solar cells are much more expensive than normal solar cells. [16]

Gallium arsenide belongs to a group of semiconductors referred to as III-V compound semiconductors. These materials can be used to produce solar cells with high efficiency but are traditionally very costly and are typically used for specialized applications such as in space. [19]

Cadmium telluride and copper indium gallium selenide are thin film technologies which achieve higher efficiencies than amorphous silicon but lower efficiencies compared to crystalline silicon. These solar cells are also more expensive than amorphous silicon solar cells. The toxicity of these solar cells is debated while amorphous silicon is considered cleaner. Cadmium telluride requires special disposal of the solar cell after its end of life due to the toxicity. [20] [21]

Perovskite solar cells contain compounds which have a perovskite structure, which is the same structure found in a mineral called perovskite ($CaTiO_3$). The cost of perovskite solar cells can potentially be made very low while reaching high efficiencies, exceeding the efficiency of crystalline silicon solar cells (the current Perovskite record efficiency is 23.3 % according to NREL [22]). At the time of writing no available products could be found, although it was noted that two companies were actively working on perovskite solar cells, namely Oxford PV and Saule Technologies [23] [24].

Quantum dot solar cells are not treated in this report because they appear to be more far from commercialization compared to the other third generation solar cells.

3.3.1 Crystalline silicon (c-Si)

Solar cells based on crystalline silicon constitute the majority of the production of solar cells (93 % share of worldwide production as of 2016) [15]. In crystalline silicon the atoms are fixed in crystal structures, and hence it is referred to as crystalline silicon. In monocrystalline silicon the silicone atoms form a single crystal structure and in polycrystalline silicone the atoms forms multiple crystal structures. Monocrystalline silicon is more expensive to produce but produces solar cells with higher efficiencies. [25] [26]

The efficiencies of commercialized crystalline silicon solar cells are between 16-21% [17] while record efficiencies in research environments reach 26.1 % [22]. Solar cells based on mono or poly- crystalline silicon require thick layers of silicon to absorb most of the light, in contrary to thin-film solar cells [17] [5].

The bandgap of crystalline silicon is approximately 1.1 eV [27], which means that photons up to a wavelength of approximately 1150 nm can excite the electrons of the silicon atoms. Solar cells based on crystalline silicon can therefore utilize a good amount of the IR part of the spectrum of sunlight.

In the production of crystalline silicon solar cells the cost of the silicon ingot which includes the growth of the fine crystal structures makes up 40-50 % of the total cost of a solar cell module. The more pure the silicon crystal is, the more expensive it is to make. The price of crystalline silicon solar cells can potentially be sensitive to shortage of silicon production in the future. [27] [5]

The lifetime of a solar cell is usually measured as the time before the solar cell output power drops to 80 % of its original value (referred to as T80). Crystalline silicon solar cells have long lifetimes usually between 25 and 30 years. [28]

3.3.2 Amorphous silicon (a-Si)

In amorphous silicon the silicon atoms do not form crystal structures, but are instead located in an irregular random order. While the atoms in crystalline silicon have four bonds to the atoms that surround them, the atoms of amorphous silicon sometimes have broken bonds which are impurities where recombination between an electron and a hole can occur. To reduce the number of broken bonds amorphous silicon is “passivated” with hydrogen atoms and the material is then called hydrogenated amorphous silicon. [27]

Amorphous silicon based solar cells have lower efficiencies compared to those based on crystalline silicon, reaching 14 % record efficiency in research environments [22] and 8-11 % for commercial cells [17]. One of the main advantages of amorphous silicon solar cells is that they are cheaper compared to crystalline silicon solar cells. Another advantage is that they require less amount of silicon and can be made thinner and mechanically flexible [27]. They can also be made in different shapes which is one of the reasons to why they are used in small electronics such as pocket calculators and watches [29].

The bandgap of amorphous silicon is between 1.6 eV to 1.85 eV [27], and hence amorphous silicon based solar cells cannot capture the same wide range of wavelengths as crystalline silicon. The bandgap levels correspond to a maximum wavelength of approximately 750 nm, which is similar to the upper limit of the human eye. Amorphous silicon solar cells therefore cannot utilize the IR part of the spectrum of the energy from the sun, as compared to crystalline silicon.

The output power of amorphous silicon solar cells is less affected by the temperature compared to solar cells based on crystalline silicon. The voltage temperature coefficient is typically half of the temperature coefficient of crystalline silicon solar cells or less. [27]

The lifetime of amorphous silicon solar cells is often reported to be around 15 years. [28]

3.3.3 Organic (OSC)

Organic solar cells consist of organic materials such as polymers, fullerenes and others [30]. An exciton is formed when an electron of an organic donor material is excited by light. In contrary to inorganic semiconductors such as silicon, the electron cannot move freely but is stuck together with the hole (together they are called an exciton). The electron and hole are separated with the help of an organic acceptor material and can then move through the external load to provide an electric current. [5] [27]

The cost of organic solar cells can be made very low since the materials are cheap and because the solar cells can be produced at high volumes in a roll-to-roll process [30]. Other attractive features of organic solar cells include the fact that they are thin, mechanically flexible and that the color can be tuned [27] [5]. Organic solar cells also perform very well in low light or indoor conditions and some sources report that they perform better than amorphous silicon solar cells in fluorescent light [31] [32].

They perform well in indoor light because the quantum efficiency is usually high for wavelengths between 350 and 750 nm [31] [27]. The quantum efficiency can however be adapted to different wavelengths by tuning the organic molecules used. For this reason there exist many different types of organic solar cells which have different properties [32]. Organic solar cells have typically not utilized IR wavelengths, but it is actively being researched and some solar cells have been demonstrated to have high quantum efficiencies up in the 800 nm range. [27] [30]

Organic solar cells are reported to have a slightly positive temperature coefficient, meaning that they perform slightly better as the temperature increases [33].

The efficiency of organic solar cells is low compared to the traditional solar cells, although as of 2016 the efficiency had been doubled in the last five years [30]. The current record efficiency of organic solar cells is 12.6 % in research environments according to NREL [22]. The efficiency of the commercially available organic solar cells from infinityPV, a Danish manufacturer of organic solar cells, is stated to be between 1.5-7 % for their demonstrator product and between 2-4 % for their “solar foil” [34].

Organic solar cells typically have shorter lifetimes compared to traditional silicon based solar cells because they suffer from different kinds of degradation and may therefore be better suited for products with an intended lifetime of a few years [30]. The degradation is reported to be especially high in outdoor conditions and is worse during the summer compared to the winter because of the increased UV radiation during the summer. The encapsulation of the solar cell is an important factor which determines how resistant the solar cell is to degradation. [33]

3.3.4 Dye-sensitized (DSSC)

Dye-sensitized solar cells contain organic dye molecules in which electrons are excited by incident light. In the excited state the electrons move to a nearby titanium dioxide (TiO_2) molecule which has a conduction band with a lower energy level. By conduction through the TiO_2 molecules the electrons reach the negative electrode and travel through the external circuit. In the meantime the missing electrons in the dye molecules have been replenished through redox reactions with an electrolyte

containing iodide (I^-). The iodide later regains the electron at the cathode when the original electron has travelled through the load. [27] [35]

This type of solar cell show very similar properties to organic solar cells even though the solar cells work in different ways [32]; they can be produced at low cost, can be made thin, mechanically flexible, and in different form factors and their color can be tuned. As with organic solar cells they are reported to perform relatively better in low light conditions and at higher temperatures compared to other solar cells [27]. The output power does also not decrease as much when the incident light has a high angle, as compared to amorphous solar cells. [35] [36]

Dye-sensitized solar cells typically have good quantum efficiency for visible light, as is also the case with organic solar cells. The dye can be optimized so that the quantum efficiency is better at utilizing certain wavelengths. A dye-sensitized solar cell can for example be better at absorbing indoor light or outdoor light, e.g. a dye from Dyenamo can utilize wavelengths up to 822 nm and can thereby capture some IR wavelengths. [36] [17] [37]

As with organic solar cells, dye-sensitized solar cells also suffer from different degradation mechanisms and hence the lifetime is shorter compared to silicon based solar cells. According to an article on website SolarEnergyForUs the lifetime of dye-sensitized solar cells is around 6 years, while G24 Power which is a manufacturer of dye-sensitized solar cells reports 3 years for their customized solar cells [28] [38]. [32]

The record efficiency for dye-sensitized solar cells in research environments is 11.9 % according to NREL [22].

3.3.5 Market investigation

To get an initial rough estimate for the cost of small solar cells, the price per area was calculated for all solar cells with an area less than 250 cm^2 available on DigiKey, a well-known electronic components distributor. The solar cell modules that were found include 23 monocrystalline silicon modules, 1 polycrystalline silicon module and 18 amorphous silicon modules from a total of 7 manufacturers. It should be noted that the price per area was calculated from the data for price per unit in combination with the area of each solar cell. While this can work as an initial estimate of the price, it must be remembered that the solar cells are sold at unit prices and that the price for a solar cell with a custom shape and area probably has a higher cost. On the other hand the unit prices are valid for a quantity of 1000 units, and could be lower for a higher quantity. The result from the price investigation is presented in Figure 5.

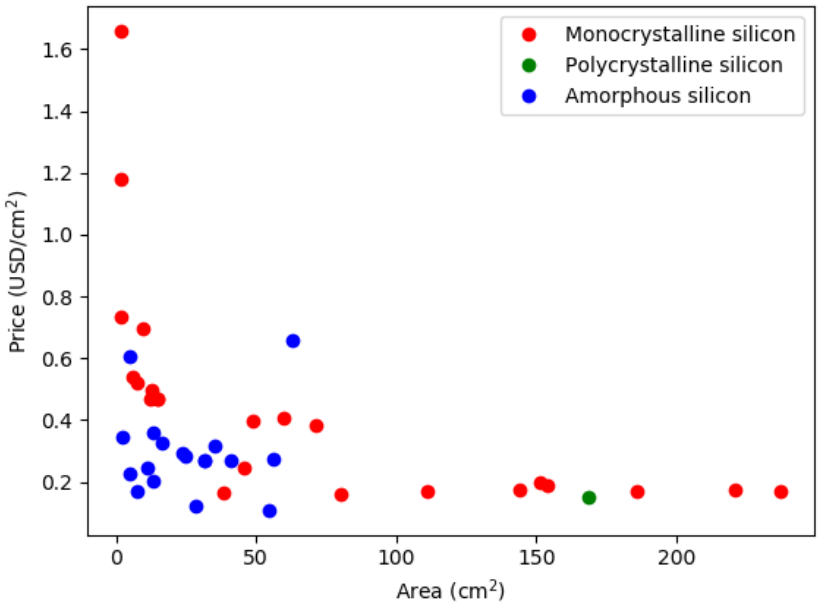

Figure 5: Result from price investigation for solar cells available on DigiKey SE on the 22nd of August 2018.

From the results it can be seen that amorphous silicon solar cells are available from approximately 0.11 USD/cm^2 and monocrystalline silicon solar cells from 0.16 USD/cm^2 (this reflects the prices for Panasonic AM-1816 and Seeed Technology 313070005). These particular solar cells have an area of approximately 55 cm^2 and 80 cm^2 respectively, and it can be seen that the prices are higher for solar cells with smaller areas.

For the third generation solar cells like organic and dye-sensitized solar cells the price is generally not publicly available since they are not sold by distributors but must be bought directly from the manufacturer.

4 ENERGY STORAGE

The power that is required by the load does not always match the power that is harvested by an energy harvesting system at every instant. This is the fundamental reason for using a rechargeable storage. If daylight is the primary source of light for a solar cell harvester then this is especially true since energy must often be stored during the day for consumption during the night. One can also imagine a system where it is acceptable to use a primary battery during the night, but to have a storage which can hold enough energy to supply the load when passing clouds block the sun for short periods of time. If the instantaneous power from the energy harvester is not enough, storage can also be required to supply power during periodic load peaks such as during radio transmission, which is common for wireless alarm nodes.

4.1 REQUIREMENTS

The following list presents important parameters for the energy storage in an energy harvesting system for wireless alarm nodes:

- **Energy density** - Alarm nodes are typically made with minimalistic designs to not be too obtrusive in a home environment. Depending on the amount of energy that is going to be stored, it is important that the energy storage has a high energy density (energy per volume).
- **Power density** – To handle the current peaks that typically occur in wireless products when they transmit data the energy storage should be able to supply enough current without the voltage dropping too low.
- **Self-discharge** – Alarm nodes usually have limited surface areas and are often placed in environments that are not necessarily well-lit, and hence the energy storage should have a low leakage current to not waste the already scarce energy. This is especially true if the energy should be stored for longer periods such as over the night or for multiple days.
- **Lifetime** – The energy storage should not have to be replaced within the lifetime of the product itself as this would effectively increase the cost of the product and in the end for the customer. It would also introduce a cost of having a service team go out to customers to replace the aged storage elements or create an inconvenience for the customer if they have to replace it by themselves.
- **Energy efficiency** – All types of energy storage has losses. Energy efficiency is defined as the ratio between the energy that is retrieved from discharging the storage and the energy that was used to charge the storage.
- **Price** – The total cost of the energy harvesting solution must be reduced as much as possible if it should be an attractive alternative to using primary batteries.

4.2 TYPES OF STORAGE

This chapter presents three common types of energy storage including capacitors, supercapacitors and batteries. Regular capacitors are typically used for storing only small amounts of energy while batteries can store large amounts for long periods. A supercapacitor has a higher energy density than normal capacitors and can tolerate more charge and discharge cycles compared to a battery [39].

4.2.1 Capacitors

A capacitor consists of two conductive plates separated by an insulating dielectric. When a capacitor is being charged, holes are collected on one side and electrons on the other. This creates a difference in potential and an electric field between the two plates. [40]

Capacitance is a measurement of the charge per voltage between the two sides, as shown in equation (4). The capacitance is proportional to the relative dielectric constant ε_r of the dielectric medium. The dielectric is polarized when exposed to an electric field, which in turn reduces the same electric field. The polarization of the dielectric is the primary way that energy is stored in a capacitor. [41]

$$C = \frac{Q}{V} \propto \varepsilon_r \tag{4}$$

The energy stored in an ideal capacitor is related to the capacitance and the voltage as described by equation (5) [40].

$$E = \frac{1}{2} C V^2 \tag{5}$$

Capacitors have a maximum voltage rating at which the dielectric separating the two plates breaks down and starts conducting [40]. The maximum voltage rating together with the capacitance sets the limit for the amount of energy that can be stored in a capacitor.

Capacitors have very low energy densities compared to supercapacitors and batteries but can charge and discharge more quickly giving them higher power densities [41] [39]. A single capacitor can only be used for storing a small amount of energy since they are normally available in the order from pF to mF range. Due to the low energy densities of capacitors it is interesting to look at supercapacitors which have higher energy densities compared to capacitors and can tolerate more charge and discharge cycles compared to batteries. [39]

4.2.2 Supercapacitors

Supercapacitors, also known as electrochemical double-layer capacitors (EDLCs), have much higher energy densities compared to normal capacitors, but also conform to equation (5) relating energy, capacitance and voltage. They exist with a capacitance range of 100 mF to over 1000 F allowing large amounts of energy to be stored [39]. The energy density of supercapacitors is lower than the energy density of batteries, but they make up for it by tolerating more charge and discharge cycles and having higher power density [39].

When a voltage is applied across the terminals of a supercapacitor, ions in the electrolyte separating the electrodes attract to the electrodes and form electric double-layers at the interfaces between electrode and electrolyte. The double-layers at these two interfaces form the capacitance in a supercapacitor. [42]

Supercapacitors can also store energy through what is known as pseudo-capacitance which involves electrochemical redox reactions between ions and the electrodes. This is more similar to how batteries store energy and can provide a higher capacitance than the electric double-layer. [41] [43]

Different ratios between double-layer capacitance and pseudo-capacitance can be achieved by choosing different materials in the design of the capacitor. Based on this ratio supercapacitors are divided into double-layer capacitors, pseudo-capacitors and asymmetric capacitors. A double-layer capacitor has a high double-layer capacitance while a pseudo-capacitor has a high pseudo-capacitance. The asymmetric capacitor, also called hybrid capacitor, has one electrode with a high double-layer capacitance and the other side with a high pseudo-capacitance. [43]

Double-layer capacitors have a breakdown voltage in the range of 2.5-3V while the breakdown voltage for hybrid capacitors can reach up to 3.8 V [42], although many cells can be put in series to allow higher voltages.

An advantage with supercapacitors is that the state of charge and the remaining energy can easily be estimated by using equation (5), something which can be challenging to do for batteries. [44] [43]

Although supercapacitors can tolerate many more charge cycles than batteries, they do also suffer from ageing effects. When a supercapacitor ages the equivalent series resistance (ESR) increases and the capacitance drops. Higher temperatures and higher operating voltages both increase the ageing rate of supercapacitors. Therefore, a supercapacitor should ideally not work close to its maximum voltage rating. According to CAP-XX, a supercapacitor manufacturer, their supercapacitors have a lifetime of approximately 50,000 hours with an unlimited number of charge and discharge cycles whereas batteries can tolerate between 150 and 1500 charge/discharge cycles. [45] [46] [39]

It is common to find the leakage current of supercapacitors stated in the datasheets as maximum leakage current after some amount of time, e.g. 72 hours. This is because the leakage current of the supercapacitor, as measured by measuring the current required to keep the supercapacitor at a constant voltage, decreases over time and eventually stabilizes [41]. The leakage current is in the range of μA/F [41] and the higher the capacitance is the higher the leakage current. The self-discharge of supercapacitors can be of significance if put in relation to the average current consumption of small wireless alarm nodes.

4.2.3 Rechargeable batteries

Rechargeable batteries are more formally known as secondary batteries while non-rechargeable batteries are known as primary batteries. A battery consists of a single or multiple electrochemical cells which may be connected in series or parallel to get the desired energy and power capacity [47].

The electrochemical cell consists of two electrodes, the anode and cathode, separated by an electrolyte. When the cell is being discharged, an oxidation reaction takes place in the anode which releases free electrons and positively charged ions. The ions can move through the electrolyte while the electrons need to take an external path through the load to end up at the cathode. In the cathode a reduction reaction takes place and the electrons are accepted. When the cell is being charged, electrons and ions instead move from the cathode to the anode. [43]

Rechargeable batteries have higher energy densities compared to supercapacitors, but lower power capacities. A disadvantage with batteries is that the capacity is reduced more quickly with the number of charge cycles compared to supercapacitors. [41] While a supercapacitor can be fully discharged to 0 V, a battery should not be discharged below a certain voltage. Batteries need to be kept within its voltage limits to operate safely and to maintain an acceptable lifetime [43]. The number of cycles that a battery can tolerate falls exponentially with the depth of discharge (DoD), which is a measure of how much of the capacity of a battery that is used in each charge/discharge cycle. The capacity of a battery should be large such that the DoD can be kept small enough to maintain a long lifetime.

Batteries generally achieve a much lower self-discharge compared to supercapacitors [48] [49] [50], and are therefore be more suited for storing energy over long periods of time. The self-discharge of lithium-ion batteries can be as low as 2 % of the full capacity per month [51].

The voltage of a battery decreases as it is discharged, but the voltage is generally more flat compared to the voltage of a capacitor. Different types of batteries are made of different materials which result in different cell voltages.

Lithium-ion batteries (Li-ion) are the most common rechargeable batteries used in consumer electronics [43] [50]. They are attractive because of their high cell voltage, usually between 3-4 V, and because of their high energy density. The cell voltage is more constant compared to other battery types for which the cell voltage can vary more widely depending on the state of charge. [43]

Before lithium-ion batteries became the dominant battery type, nickel metal-hydride (NiMH) batteries were commonly used in portable electronics. They are still widely used, but are being replaced by more energy dense lithium-ion batteries. The cell voltage of nickel metal-hydride batteries is lower compared to lithium-ion batteries, at approximately 1.2 V. The voltage of nickel metal-hydride batteries can decrease if the battery is repeatedly partially charged, a phenomenon known as voltage depression. The capabilities of the battery can however be restored by occasionally doing a full discharge of the battery. [43] Considering the use of NiMH in energy harvesting applications where the battery can be repeatedly partially charged depending on the intermittence of light, this property should be considered.

Batteries have a more narrow operating temperature than supercapacitors (-20 to +65°C for batteries vs -40 to +85°C for supercapacitors according to [39]), and must be kept within its limits to maintain safety and minimize ageing and damage to the battery. For wireless alarm nodes which may be placed in window locations or in houses with no temperature regulation the maximum and minimum ambient temperature needs to be considered for the whole year and for the different geographical regions where the product is used. Lithium based batteries are especially sensitive to temperature and temperature monitoring is often used to ensure safe operation. [43]

When batteries are charged the current should be limited to not cause overcharging, which can happen when the charging rate is faster than the chemical reactions. Charging too fast can cause a rise in temperature, damage to the cell or a loss of energy. The charger should be able to charge the battery at a good rate but within the limits and know when to stop charging the battery. Different methods for charging exist and a common one is the CCCV method (constant current constant voltage). The CCCV method achieves a high charging rate with the constant current phase but prevents charging the battery too much with the constant voltage phase in which the charging current gradually decreases. [43]

The energy efficiency of both lithium-ion batteries and supercapacitors reach high values, often between 85-100 %. The efficiency typically varies depending on how fast the medium is charged or discharged, lower charging rates achieving higher efficiencies. Supercapacitors are often reported to reach higher efficiencies compared to lithium-ion batteries. [52] [53] [54]

4.2.4 Market investigation

The webshop of DigiKey was scanned for supercapacitors in the range of 0-5 F to collect prices for such capacitors. Table 2 presents the results of the price scan for the range of capacitances divided into five intervals. The price is shown both for capacitors with a lower voltage rating and for capacitors with a higher voltage rating achieved by packing two cells into a single module.

Table 2: Prices of supercapacitors between 0.1-5 F collected from DigiKey[1].

Capacitance (F)	**Available from, price per unit (USD) / 1 ku**		**Calculated price per energy capacity[2] (USD/Wh)**	
	Rated voltage 2.5-3 V	**Rated voltage 5.0-5.5 V**	**Rated voltage 2.5-3 V**	**Rated voltage 5.0-5.5 V**
0.1-0.99 F	0.42	0.73	339.39-4834.4	175.51-2102.4
1-1.99 F	0.33	1.15	132.66-380.16	137.54-331.2
2-2.99 F	0.41	1.44	109.70-236.16	114.63-207.36
3-3.99 F	0.50	2.02	100.25-192	120.50-193.2
4-5 F	0.71	3.23	113.6-232.56	153.76-232.56

A similar price scan for rechargeable batteries was made on DigiKey, although it was found that the price varies widely amongst products of the same technology and of the same capacity. It is likely necessary to contact manufacturers directly to get more usable information about their selection and prices. Table 3 shows a list of different batteries and battery-like devices and their respective cost.

[1] Price from DigiKey US, https://www.digikey.com/, accessed 21th of August 2018.

[2] Energy capacity calculated by assuming an operating voltage between 0 V and the rated voltage.

Table 3: Prices of a selection of rechargeable batteries collected from DigiKey[3] US on the 21th of August 2018.

Product	**Type**	**Nominal capacity (mAh)**	**Nominal voltage (V)**	**Typical current**	**Available from, price per unit (USD) / 1 ku**	**Calculated price per energy capacity (USD/Wh)[4]**
Various lithium coin cells 23-30 mm diameter	Lithium	30-100	3	µA	2.04	6.80-22.67
SparkFun 18650	Lithium-ion	2600	3.7	mA to A	5.95	0.62
FDK America HR-3U-2500 AA	NiMH	2300	1.2	mA to A	3.30	1.20
Murata UMAC	Lithium-ion based (unconventional [55])	3	2.3	µA to mA	3.24	469.57
Murata UMAL	Lithium-ion based (unconventional [55])	24	2.3	µA to mA	12.46	225.72
Panasonic Pin-type CG-320A	Lithium-ion	15	3.8	µA to mA	4.31[5]	75.61

When comparing the price per energy capacity for supercapacitors and batteries it can be seen that the price of supercapacitors is generally higher compared to batteries. The exception seems to be for the Murata UMAC and UMAL devices, which are on par or more expensive compared to supercapacitors, although it is for these devices questionable if they can be counted as batteries or not, see reference [55].

An investigation based on another dataset was made to see how the energy density of supercapacitors and batteries compared. The energy density of 18 supercapacitors of three different brands in the range of 0.1-15 F was found to be between 0.3 Wh/L and 4.1 Wh/L when assuming that the supercapacitor could be used in the whole voltage interval from 0 V up to the rated voltage. A similar investigation was made of 10 different batteries of three different brands in the range of 3-2350 mAh capacity, and it was found that the energy density was in between 45 Wh/L and 500 Wh/L. This suggests that the energy density for li-ion batteries and supercapacitors can differ by a factor of 100.

[3] Price from DigiKey US, https://www.digikey.com/, accessed 21th of August 2018.
[4] Energy capacity estimated as nominal voltage (V) multiplied by nominal capacity (Ah).
[5] Price from Octopart, for seller Rutronik, accessed 21th of August 2018.

5 POWER ELECTRONICS

A typical energy harvesting system for solar cells includes two voltage converters; one at the input and one at the output [56], as shown in Figure 6. The DC-DC converter at the input is used to charge the rechargeable storage and to make the solar cells operate at the MPP of the I-V curve. The latter is known as maximum power point tracking (MPPT) and is further explained in the following subchapter. The second stage where a voltage converter is typically used is between the rechargeable storage and the load. If the rechargeable storage is a capacitor the voltage varies with the state of charge and a regulated DC-DC converter is required to stabilize the voltage across the load. Even batteries that work at a fairly constant voltage can require a DC-DC converter if there is a mismatch between the battery voltage and the voltage requirements of the load, but also to have the load work at the optimal voltage which minimizes power consumption.

Figure 6: Typical energy harvesting system with solar cells as input source.

5.1 MAXIMUM POWER POINT TRACKING

For the solar cells to operate in the MPP and extract maximum power, it is as previously mentioned required to match the load impedance to the impedance of the solar cell in the MPP. Since the current and voltage from a solar cell depends on the light conditions, the load impedance matching needs to be done continuously. Making the solar cells operate in the MPP is achieved through maximum power point tracking (MPPT).

The DC-DC converter between the solar cell module and the rechargeable storage is usually a switched buck or boost converter [56]. A boost converter is used if the solar cell module has a lower voltage than the rechargeable storage. If instead the solar cell module has a higher voltage than the rechargeable storage a buck converter is used as it steps down the voltage. By controlling the duty cycle of the converter the ratio between the voltage at the input and the voltage at the output of the converter can be changed. The output voltage is fixed by the voltage of the rechargeable storage and so the duty cycle can be used to control the input voltage which is the voltage across the solar cell module. In this way it is possible to control the operating point of the solar cell.

A simple way to perform MPPT is to assume that the voltage at the MPP is a constant fraction of the open-circuit voltage, a method which is known as the Fractional Open Circuit Voltage method (F.OCV) [57]. The fraction of the OCV at which the MPP is located differs between different types of solar cells, therefore chips which use this type of MPPT often makes it possible to set the fraction e.g. through a voltage division resistor network. The bq25504 energy harvesting IC from Texas Instruments which implements this method periodically measures the OCV by temporarily disconnecting the solar cell module from the load [58].

Another group of methods are the hill climbing power point trackers. These methods have in common that they adjust the load in steps and measure how the output power is affected. The goal is to move along the I-V curve until the MPP is found. Two common methods in this category are the Perturb & Observe (P&O) and the Incremental Conductance (IC) methods. [57]

5.2 ENERGY HARVESTING CHIPS

There are integrated circuits which contains the necessary functionality that is typically required in an energy harvesting system. Common functionality of such chips includes:

- Charging of rechargeable storage
- MPPT
- Output voltage regulation
- Automatic switching to backup battery

The next section gives a description of the bq255xx series energy harvesting chips from Texas Instruments to show a more concrete example of the functionality of such chips. Next a list of prices of energy harvesting chips with MPPT is presented to show what the typical price is.

5.2.1 bq255XX series from Texas Instruments

The bq255XX series from Texas Instruments includes three integrated circuits with boost converters and battery management for ultra-low power energy harvesting applications [59]. MPPT is achieved through the F.OCV method and the fraction is programmable by choosing the values of resistors in a voltage division network. The controller samples the OCV every 16 s by temporarily disconnecting the solar cells. [58]

When a discharged rechargeable storage is connected to the IC, the circuit operates in cold-start mode which means that the boost converter is unregulated and works at a lower efficiency. When the storage is charged to approximately 1.7 V, the circuit enters the main mode and the boost converter can work according to the MPPT scheme with a high efficiency. The voltage interval in which the rechargeable storage is connected to the load is programmed by a set of resistors forming another voltage division network. [58]

The integrated circuit comes in three variants with slightly different functionality, the bq25504 being the most basic model includes the functionality described above. The bq25505 also includes two gate drivers which can be connected to the gates of two transistor switches to automatically switch to a backup battery when the voltage of the rechargeable storage decreases below the programmed level. The bq25570 has in addition to the features of the bq25504 a buck converter on the output to provide a regulated output voltage. [60] [61]

5.2.2 Market investigation

To get a range for the price of energy harvesting chips with MPPT functionality, prices were collected from the respective website of three manufacturers and presented in Table 4. The table is made for the purpose of getting a rough estimate of the price of energy harvesting chips and is not made for comparing the functionality of different chips.

Table 4: Prices of energy harvesting chips with MPPT functionality.

Manufacturer	Product name	Price per unit (USD)
Texas Instruments	bq25504	2.05 USD / 1 ku[6]
	bq25505	2.25 USD / 1 ku[6]
	bq25570	3.20 USD / 1 ku[6]
Analog Devices	ADP5090	1.99 USD / 1 ku[7]
	ADP5091	2.49 USD / 1 ku[7]
	ADP5092	2.49 USD / 1 ku[7]
	LTC3105	2.70 USD / 1 ku[7]
	LTC3106	2.94 USD / 1 ku[7]
STMicroelectronics	SPV1040	3.10 USD / 1 ku[8]
	SPV1050	2.99 USD / 1 ku[9]

From Table 4 it is seen that the price for the chips lie roughly in the range of 2-3 USD per unit for a quantity of 1000 units, not counting the external components that are required. The external components that are required generally include an inductor for the switched converter, capacitors and resistors. A breakdown of the cost of an energy harvesting solution based on the bq25505 can be found in chapter 7.6.

5.3 Solutions without MPPT

While MPPT ensures that the solar cells operate in the MPP it increases the cost of the product and introduces losses in the system via the converter and control logic. It should also be considered if it is possible to get good efficiency from the system through a design where the solar cells and rechargeable storage are carefully selected such that they naturally work at an acceptable level of efficiency without MPPT.

If the energy storage medium has a fairly constant voltage, which is the case for many batteries, the solar cell and battery can be selected such that the battery voltage is close the MPP of the solar cell [50]. This does not guarantee that the solar cells operate at MPP in the same way as MPPT does since it does not react to changing light conditions, but with a good design it can provide good efficiency at a reduced cost.

An example of an energy harvesting solution with a backup battery but without MPPT is shown in Figure 7. The solar cell module charges the C1 capacitor which is used as rechargeable storage. When the C1 capacitor is charged above 3 V plus a diode drop, the D1 diode is forward biased and the D2 diode is blocking, and so the rechargeable storage is used to power the load. If the C1 capacitor has not been charged enough, the D1 diode is blocking and the D2 diode is forward biased so that the backup battery powers the load. A voltage regulator is put on the output to get a stable voltage across the load. The maximum voltage that the C1 capacitor is charged to is defined by the OCV of the solar cell module. Since there is no boost converter between the solar cell module and the rechargeable storage, the solar cell must have a high OCV to be able to store sufficient energy in the capacitor without requiring a too high capacitance.

[6] Price from Texas Instruments, http://www.ti.com/power-management/battery-management/energy-harvesting/products.html, accessed 2018-07-10.
[7] Price from Analog Devices, http://www.analog.com/en/parametricsearch/11503, accessed 2018-07-10.
[8] Price from STMicroelectronics, https://www.st.com/content/st_com/en/products/power-management/photovoltaic-ics/mppt-dc-dc-converters/spv1040.html#samplebuy-scroll, accessed 2018-07-10.
[9] Price from STMicroelectronics, https://www.st.com/content/st_com/en/products/power-management/photovoltaic-ics/mppt-dc-dc-converters/spv1050.html#samplebuy-scroll, accessed 2018-07-10.

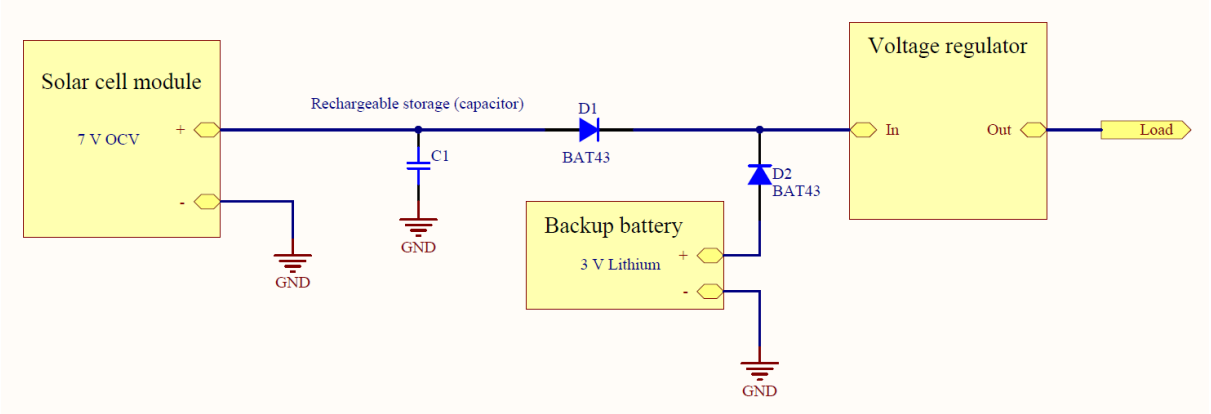

Figure 7: Energy harvesting solution with backup battery but without MPPT. [10]

An estimate of the cost of the energy harvesting solution in Figure 7 excluding the rechargeable storage is shown in Table 5. As can be seen in the table the cost of this solution is at least 10 times lower compared to an energy harvesting chip, not even counting the external components that are required by the energy harvesting chip.

Table 5: Estimate of the cost of the energy harvesting circuit in Figure 7.

Designator(s)	**Part**	**Quantity**	**Price per unit (USD)**
Energy harvesting circuit			0.30
D1, D2	ON Semiconductor BAT43XV2	2	0.02 / 200 ku[11]
Voltage regulator	Torex Semiconductor Ltd XC6201P302PR-G[10]	1	0.26 / 1 ku[11]

[10] Based on schematic provided by engineer with experience with solar cells.
[11] Price from DigiKey SE, https://www.digikey.se/, accessed 2018-07-17.

6 MEASUREMENTS

To evaluate the potential of using solar cells it is desirable to measure the output power in the environment where they will be used, particularly since it can be hard to estimate the output power based on the information found in datasheets.

Measurements were done in a home environment at two typical locations for the magnet contact alarm node; in windows and at the inside of front doors. The home environment measurements were made with sunlight as the only source of light. These measurements are supplemented by separate measurements made in a lab environment investigating how much power the solar cells produce in artificial light.

The goal of the measurements is to compare the performance of different solar cells in different locations, mounting directions and with different light sources. The aim is also to make a rough estimation of the amount of energy that can be harvested.

6.1 SOLAR CELL MODULES FOR EVALUATION

Three different types of solar cell modules were selected to be evaluated in the measurements, as listed in Table 6. The amorphous silicon and organic solar cell module were selected because they are deemed to be interesting for low cost energy harvesting applications, based on the information in chapter 3. These are compared to a monocrystalline silicon module, which is typically more expensive but has a higher efficiency. The silicon based solar cells were bought from a distributor of electronic components while the organic solar cell module is a prototype provided by a manufacturer.

Table 6: Solar cell modules selected for the measurements.

Product name	**Type**	**Indoor/outdoor optimized**	**Configuration**	**Area (cm^2)**	**OCV (V)**
IXYS SLMD121H04L	Monocrystalline silicon	Good for both	4 cells in series	6.02	2.5
Panasonic AM-1417CA	Amorphous silicon	Indoor	4 cells in series	4.87	2.4
Organic solar module prototype	Organic	Indoor	6 cells in series	14.70	4

6.2 MEASUREMENTS IN HOME ENVIRONMENT

The measurements in the home environment were made using an Arduino in combination with an analog circuit which acts as a variable load connected to the solar cell module. This allows the I-V curve of the solar cell to be captured by the Arduino and sent to a PC for further analysis. See appendix A for a full description of the measurement setup.

In the following measurements, the I-V curve was continuously captured throughout the day, so that the harvestable energy could be estimated by integrating the instantaneous power over time. In the following graphs, the power over time in the MPP of each I-V curve is presented. Each curve also shows the illuminance experienced by the solar cell module as measured by a lux meter.

The measurements were made in a house in southern Sweden. During the measurements the indoor temperature was in the range of 18-25° C.

6.2.1 Window location

The three solar cell modules were evaluated in two windows, one facing approximately north-west and the other facing south-east. The windows are normal glass windows and have not been designed to block IR wavelengths (the windows are not low-E windows). Since the magnet contact alarm node has different surfaces facing different directions and due to the fact that it can be mounted in different locations in a window, two ways of mounting the solar cell modules were tested in the measurements, as shown in Figure 8.

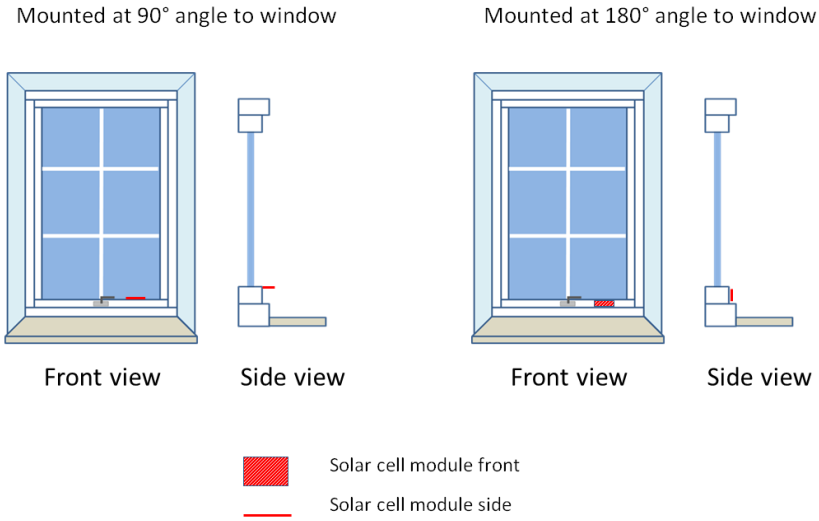

Figure 8: The two ways the solar cell modules are mounted in the window measurements.

The layout of the room and the position of the windows are shown in Figure 9.

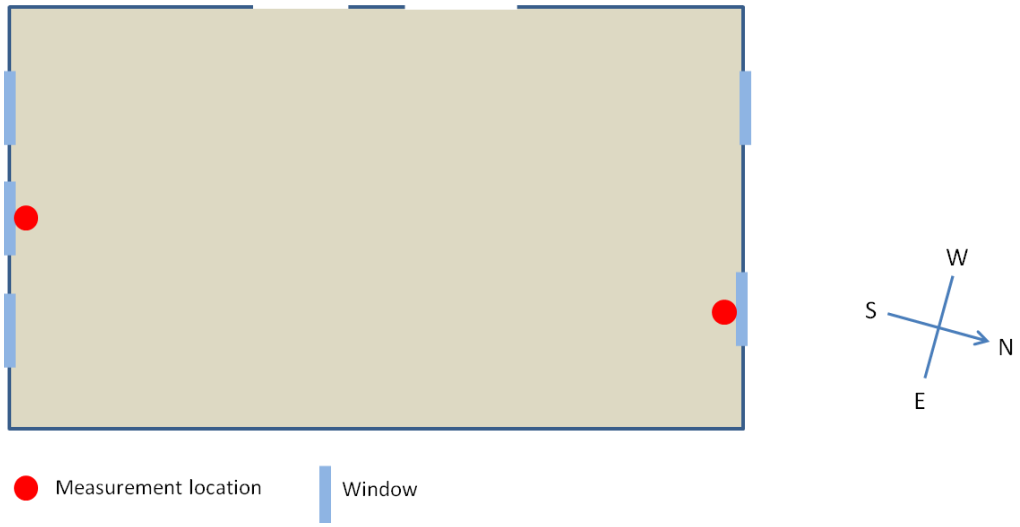

Figure 9: Layout of the room where the window measurements are done.

The conditions for the measurements are listed in Table 7.

Table 7: Conditions for the measurements on the 24th of May 2018.

Date	**Sunrise and sunset (CEST)**	**Weather conditions**	**I-V curve sampling interval (min)**	**Current sense resistor (Ω) (see appendix A)**
2018-05-24	04:41, 21:28	Cloud free (sunny)	60	Varied between 100 and 1463

The maximum power over time in the north-west window can be seen in Figure 10 for a 90° mounting angle and in Figure 11 for a 180° mounting angle. The equivalent measurements in the south-east window are shown in Figure 12 and Figure 13.

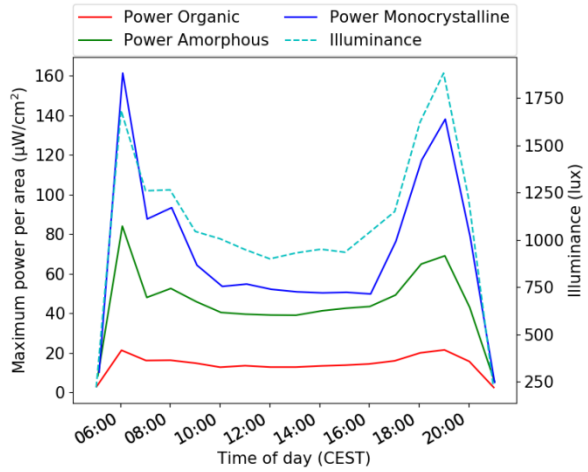

Figure 10: Maximum power per area over time for NW window with solar cell mounted at a right angle from the window (90°).

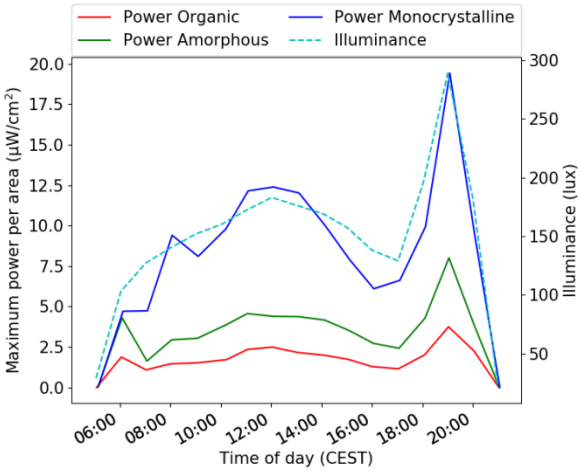

Figure 11: Maximum power per area over time for NW window with solar cell mounted behind the window frame (180°).

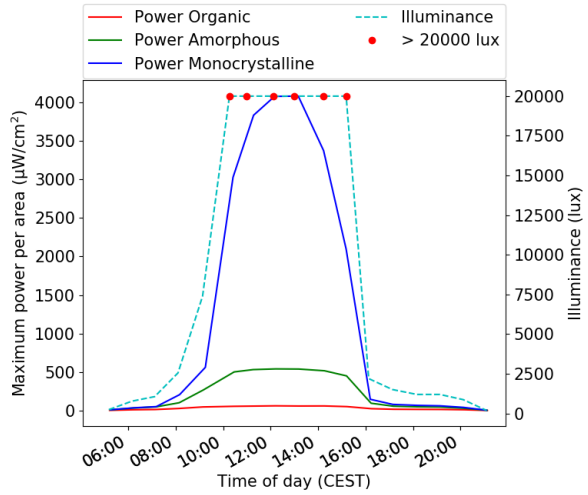

Figure 12: Maximum power per area over time for SE window with solar cell mounted at a right angle from the window (90°).

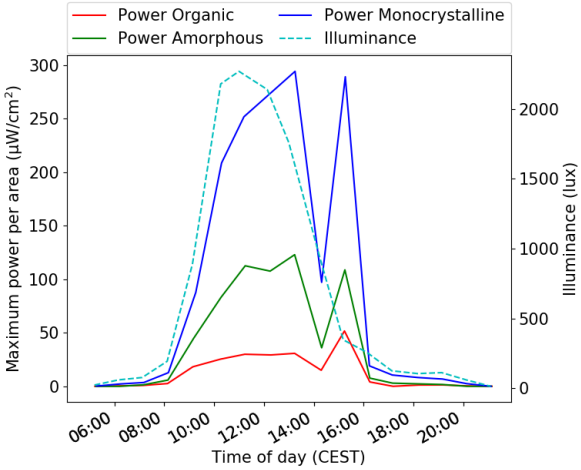

Figure 13: Maximum power per area over time for SE window with solar cell mounted behind the window frame (180°).

Note that the different curve forms seen in the figures above is the result of them being located in different windows facing different directions and because they are oriented in different ways. For example Figure 10 shows peaks in the morning and evening since it is facing north-west while Figure 12 shows a single peak at the middle of the day since it is facing south-east. Reflections in window board, furniture and other objects also seem to play a big role, which can be seen by the difference in scale of the curves in Figure 11 and Figure 13 which both shows cases for when the solar cells where facing inwards towards the room, but for different windows. The proximity of the neighboring houses also plays a role since they cover the Sun at different times and also provide a good amount of reflection depending on the paint of the houses.

The maximum harvestable energy for the whole day calculated by integrating the maximum power over time can be found in Table 8 for both windows and mounting angles.

Table 8: Maximum harvestable energy per area on the 24th of May 2018.

Window	Mounting angle	Maximum harvestable energy per area for the whole day (Ws/cm^2)		
		Organic solar cell module	Amorphous solar cell module	Monocrystalline solar cell module
North-west	90°	0.8596	2.6855	4.2367
North-west	180°	0.1034	0.2079	0.5113
South-east	90°	1.9562	13.7092	76.6322
South-east	180°	0.7640	2.3066	5.6297

6.2.2 Front door location

The three solar cell modules are also evaluated on the inside of two front doors of the house. Again, the magnet contact can be mounted in different ways. The magnet contact alarm node is most often placed on the door frame and the permanent magnet is often placed on the door itself, however the opposite is also possible. When the sensor is placed on the door frame, the largest plane of the sensor is facing a direction perpendicular to the plane of the door, from here on referred to as the "frame plane". If the sensor is instead placed on the door, the largest plane of the sensor is instead facing the same direction as the door plane. The direction that the sensors largest plane faces for the two cases is shown in Figure 14.

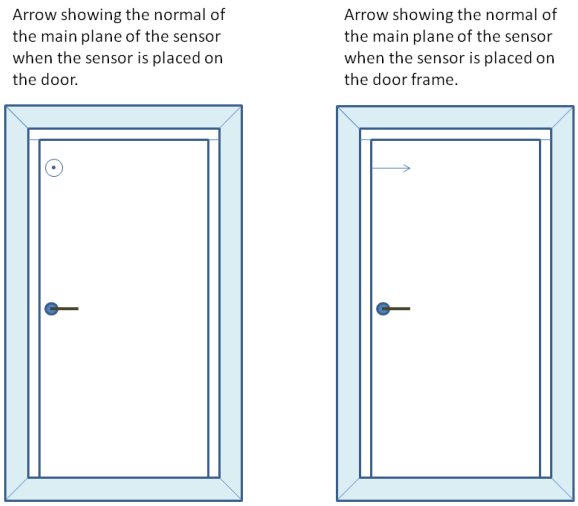

Figure 14: Shows the direction that the main plane of the sensor is facing when the sensor is placed on the door and on the frame.

The conditions for the measurements are listed in Table 9.

Table 9: Conditions for the measurements on the 9th of May 2018.

Date	Sunrise and sunset (CEST)	Weather conditions	I-V curve sampling interval (min)	Current sense resistor (Ω) (see appendix A)
2018-05-09	05:08, 21:01	Cloud free (sunny)	60	4550

The two front doors where the measurements took place are referred to as front door 1 and front door 2. The layout of the room with front door 1 is shown in Figure 15 and the layout of the room with front door 2 in Figure 16.

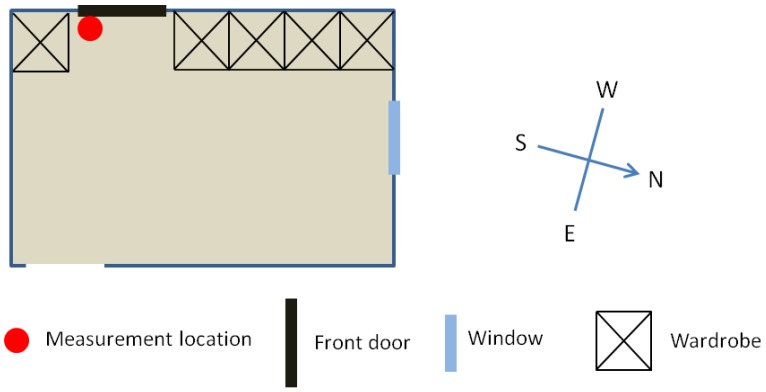

Figure 15: Layout of the room with front door 1.

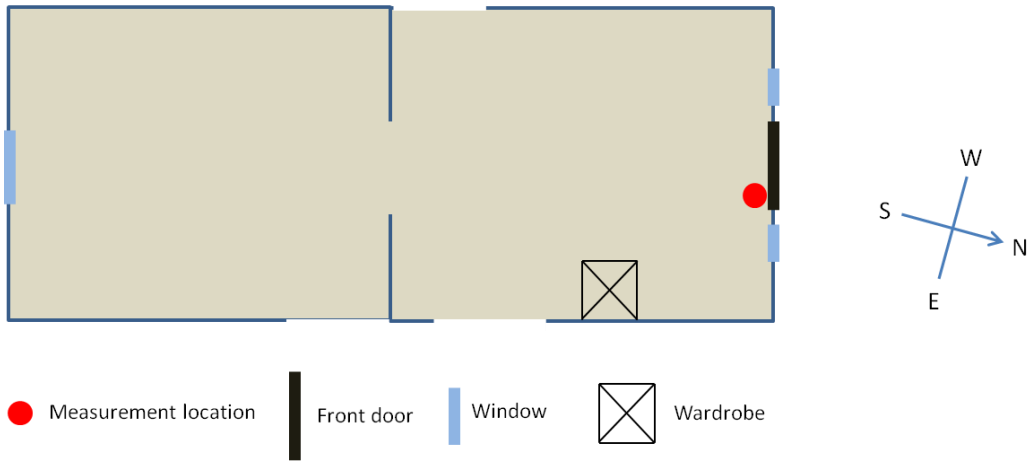

Figure 16: Layout of the room with front door 2 and layout of connecting room showing that the door is in parallel with a window.

The maximum power over time at front door 1 is shown in Figure 17 when the solar cell modules are mounted on the door plane and Figure 18 when mounted on the frame plane. The equivalent measurements for front door 2 are shown in Figure 19 and Figure 20.

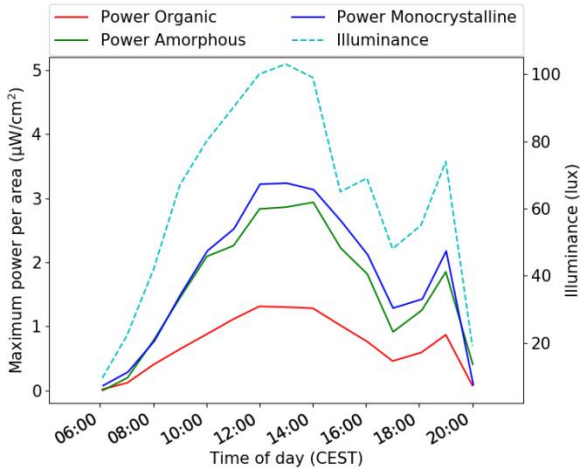

Figure 17: Maximum power per area over time for front door 1 at the door plane.

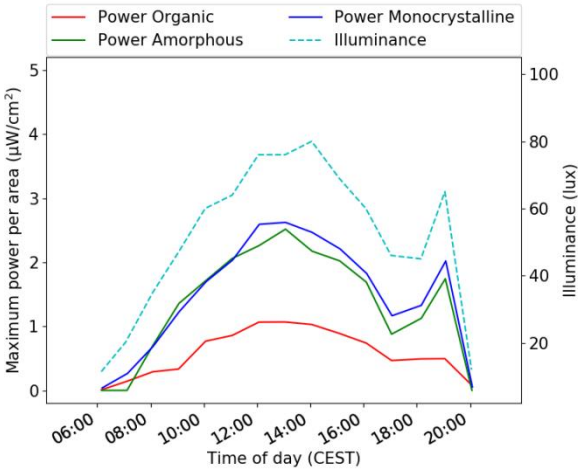

Figure 18: Maximum power per area over time for front door 1 at the frame plane.

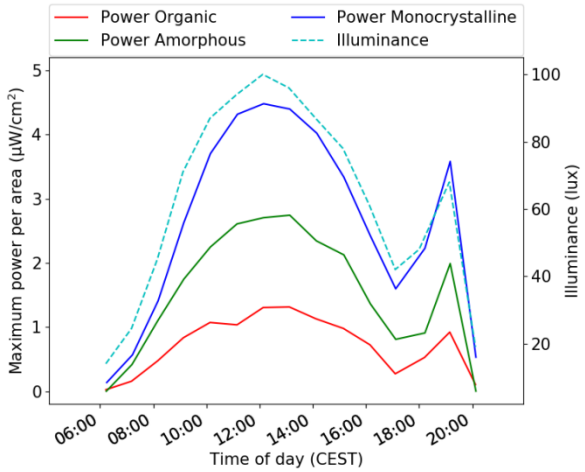

Figure 19: Maximum power per area over time for front door 2 at the door plane.

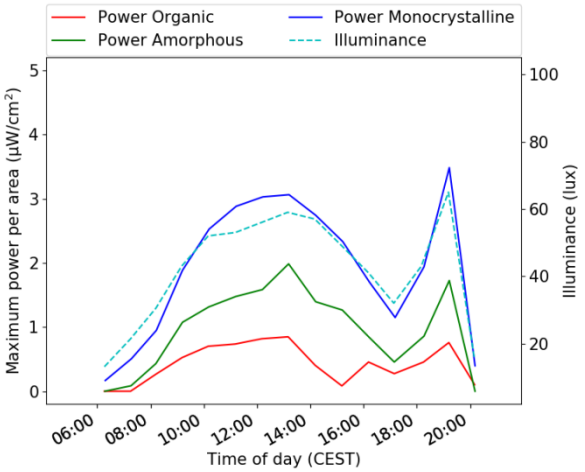

Figure 20: Maximum power per area over time for front door 2 at the frame plane.

The maximum harvestable energy for the whole day calculated by integrating the maximum power over time can be found in Table 10 for both front doors and both mounting planes.

Table 10: Maximum harvestable energy per area on the 9th of May 2018.

Front door	**Mounting plane**	**Maximum harvestable energy per area for the whole day (Ws/cm²)**		
		Organic solar cell module	**Amorphous solar cell module**	**Monocrystalline solar cell module**
1	Door	0.0388	0.0852	0.0955
1	Frame	0.0312	0.0727	0.0797
2	Door	0.0387	0.0828	0.1398
2	Frame	0.0228	0.0519	0.1019

6.2.3 Comparison of sunny and cloudy day

Two earlier measurements made on the organic solar cells mounted in the two already described windows at 90° mounting angle is presented here to show the difference between a sunny and a

cloudy day in April. Although many different levels of cloudiness exist, these measurements are made to give an example of how the harvestable energy is affected. The measurements were made in the same room as the previously discussed window measurements.

The conditions for the measurements in the window location are listed for both days in Table 11.

Table 11: Conditions for the measurements on the 9th of May 2018.

Date	**Sunrise and sunset (CEST)**	**Weather conditions**	**I-V curve sampling interval (min)**	**Current sense resistor (Ω) (see appendix A)**
2018-04-09	06:18, 20:01	Cloud free (sunny)	30	1463
2018-04-25	05:39, 20:33	Cloudy with rainfall	30	1463

The measurements on the sunny day 9th of April for the north-west window are shown in Figure 21 and for the south-east window in Figure 22.

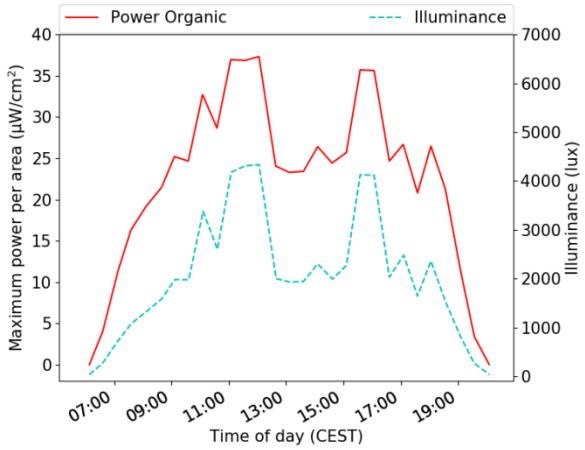

Figure 21: Maximum power per area over time for the NW window on the sunny day 9th of April 2018 (90° mounting angle).

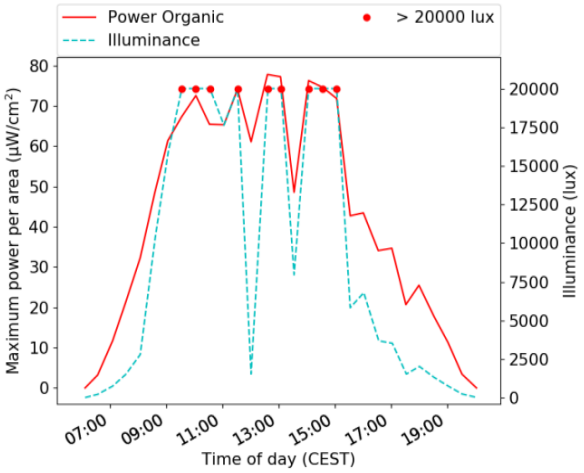

Figure 22: Maximum power per area over time for the SE window on the sunny day 9th of April 2018 (90° mounting angle).

The measurements on the cloudy day 25th of April for the north-west window are shown in Figure 23 and for the south-east window in Figure 24.

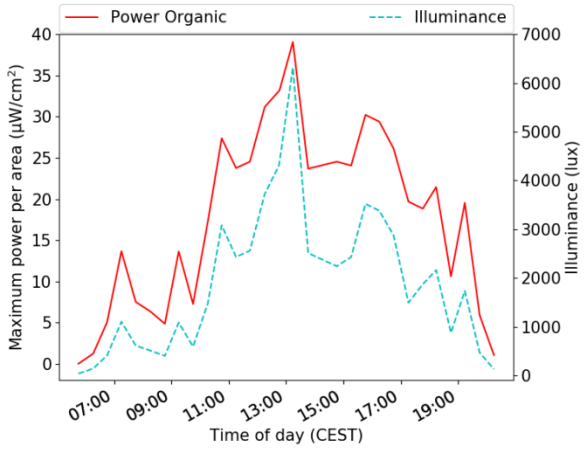

Figure 23: Maximum power per area over time for the NW window on the cloudy day 25th of April 2018 (90° mounting angle).

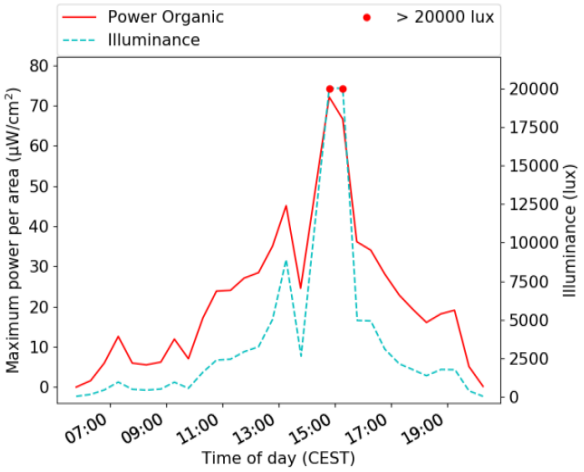

Figure 24: Maximum power per area over time for the SE window on the cloudy day 25th of April 2018 (90° mounting angle).

The maximum harvestable energy for each day calculated by integrating the maximum power over time can be found in Table 12.

Table 12: Harvestable energy on the sunny day 9th of April 2018 and the cloudy day 25th of April 2018 when working at MPP.

Weather condition	**Maximum harvestable energy per area for the whole day (Ws/cm²)**	
	NW window	**SE window**
Sunny day (9th of April 2018)	1.1631	2.2330
Cloudy day (25th of April 2018)	1.2014	0.9611

6.3 MEASUREMENTS IN LAB ENVIRONMENT

The measurements in the lab environment were made using the N6705 DC Power Analyzer from Keysight Technologies. The I-V curves for the solar cell modules were measured by programming the N6705 to increase the current linearly while measuring the voltage and current. When the I-V curves were captured they were transferred to a PC and the MPP of each I-V curve was found. The voltage measurements were made with an accuracy of ≤ 2.45 mV while the current measurements were made with an accuracy of ≤ 10.4 µA for currents above 1 mA and an accuracy of ≤ 350 nA for currents below 1 mA.

6.3.1 Performance in artificial light

The three solar cell modules were tested in the light from the three sources of artificial lighting which are listed in Table 13. All measurements were performed in a room which had an illuminance of 0.01 lux when the artificial light source was turned off, which was considered dark enough to not affect the measurements. The ambient temperature in the lab room was measured to 24.5° C. The distance between the solar cell modules and the light source was varied, effectively varying the illuminance at the solar cell modules, so that graphs showing the maximum power as a function of illuminance could be created. Because the lamps were connected to a 50 Hz wall outlet, the captured IV curves had to be filtered with a moving average filter before the MPP could be found. The illuminance was measured using a lux meter.

Table 13: LED, CFL and Halogen lamps used in the experiment.

Lamp	Type	Color temperature	Lumen (lm)	Power rating
Ledsavers Globlampa E27	LED	2700 K	806	9 W (≈ 60 W)
Osram Duluxstar E27	CFL	2700 K	825	11 W (≈ 60 W)
Osram Classic Superstar E27	Halogen	2700 K	700	46 W (≈ 60 W)

The measurement results showing the maximum power for the three solar cells for the three types of artificial lights are shown in Figure 25, Figure 26 and Figure 27.

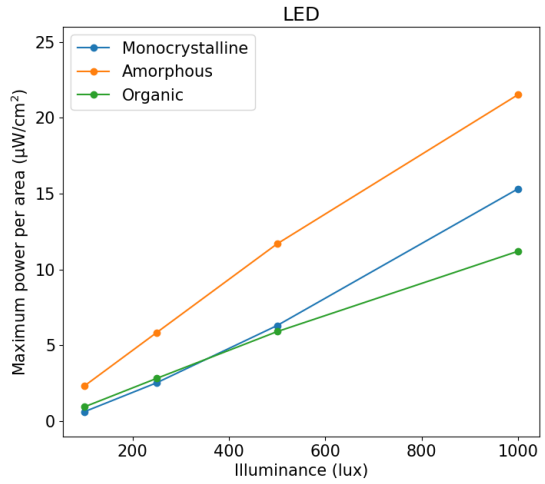

Figure 25: Maximum output power of the three solar cell modules in the light from a LED lamp.

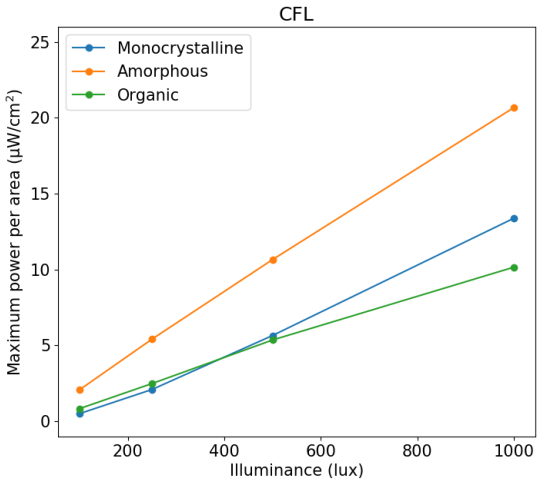

Figure 26: Maximum output power of the three solar cell modules in the light from a CFL lamp.

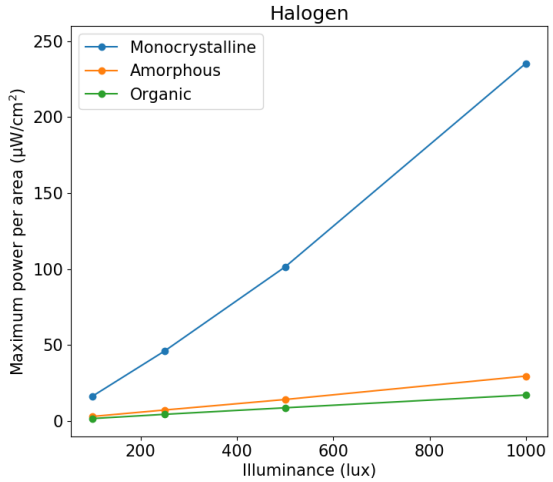

Figure 27: Maximum output power of the three solar cell modules in the light from a halogen lamp.

The distance between the solar cell modules and the light source is shown for each level of illuminance in Table 14.

Table 14: Distances between lamp and solar modules for each level of illuminance for all three lamps.

Illuminance (lux)	**Distance between lamp and solar cell module (cm)**		
	LED lamp	**CFL lamp**	**Halogen lamp**
100	105.5	94.5	125.0
250	60.0	56.5	65.5
500	42.0	39.0	43.5
1000	30.5	28.0	30.5

By assuming that the lamps are turned on for 24 hours a day, the energy that can be harvested each day is calculated by multiplying the measured power by 24 hours. This energy is presented in Figure 28, Figure 29 and Figure 30.

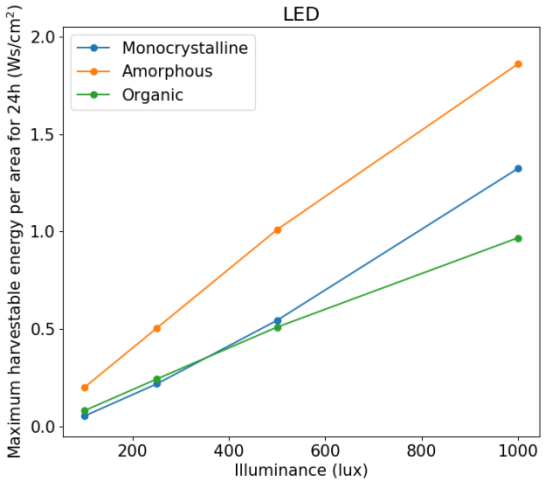

Figure 28: Maximum harvestable energy for 24h in the light of a LED lamp.

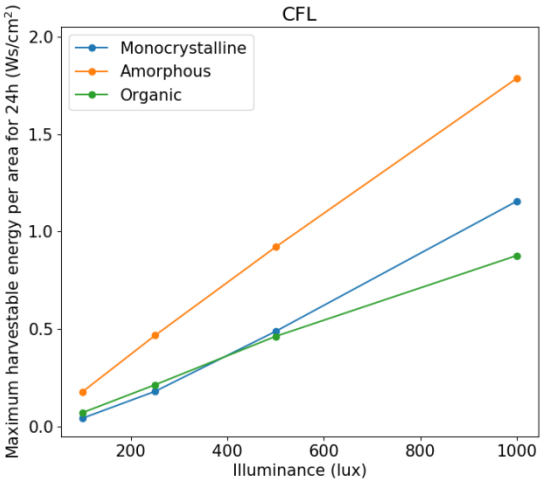

Figure 29: Maximum harvestable energy for 24h in the light of a CFL lamp.

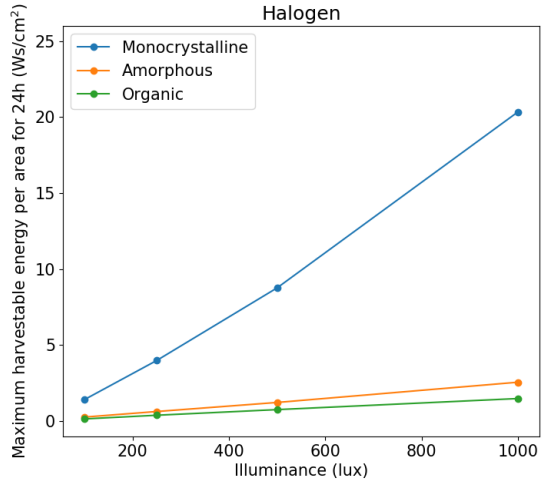

Figure 30: Maximum harvestable energy for 24h in the light of a halogen lamp.

7 PROTOTYPE

To demonstrate how solar cells can be used to power a wireless alarm node a prototype was built for Verisure's existing magnet contact node. The magnet contact has low power consumption and is used on windows which provide good light conditions.

The solution for harvesting energy was built based on the bq25505 energy harvesting chip from Texas Instruments. The solution includes a supercapacitor used for storing energy that is harvested during the day so that it can be consumed during the night. To make sure that the alarm node can function even during times when the harvested energy is not enough, the solution also includes a primary battery which is used for backup power (CR2025 lithium coin cell battery). An organic solar cell module manufactured to fit the plastic casing of the magnet contact node was used for harvesting light.

The energy harvesting solution was then connected to the power terminals of a magnet contact, which is otherwise normally powered by two AAA batteries. A system overview of the prototype can be seen in Figure 31.

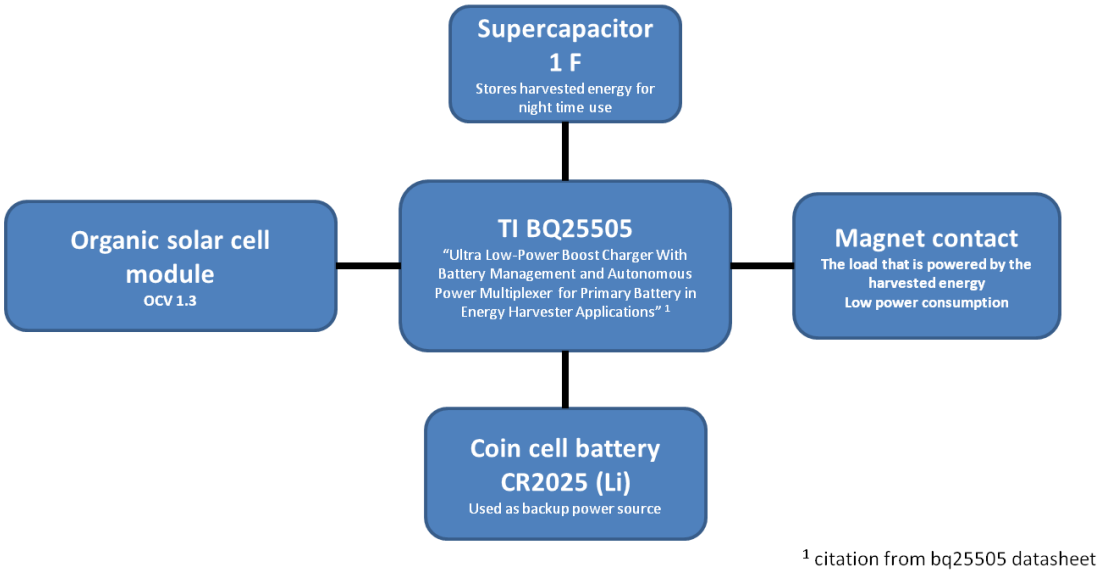

Figure 31: Overview of the energy harvesting system built for the prototype.

The following chapters include a description of the magnet contact node and a more in depth description of the prototype that was built.

7.1 MAGNET CONTACT

The magnet contact node is used on windows or doors to detect if the window/door is closed or open. The detection mechanism consists of a permanent magnet placed on either the window/door itself or on the frame which is fixed to the walls of the house. The magnet contact sensor is then placed on the opposite option, either the window/door or on the frame. When the window/door is opened the magnetic field sensed by the magnet contact sensor changes, and the detection mechanism is achieved.

The approximate shape of Verisure's magnet contact sensor along with the area of each surface is shown in Figure 32.

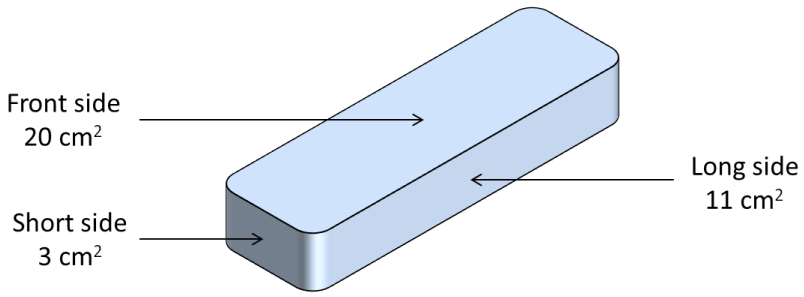

Figure 32: Approximate shape of Verisure's magnet contact sensor.

The average power consumption of the magnet contact is less than 50 µW, which means that the device consumes less than 4.32 Ws per day. Two AAA batteries connected in series are normally used to power the device. The alarm circuit contains a voltage regulator on the input to control the voltage over the rest of the circuit. While the average power consumption of the device is low, the current drawn by the device increases substantially during radio transmission which occurs periodically.

7.2 SOLAR CELL MODULE

Both the long side and the front side of the magnet contact sensor were considered when deciding which surface to put the solar cells on. When the magnet contact sensor is mounted on a window, the front side forms a 180° angle to the window such that the front side surface faces towards the room away from the window. The long side instead forms a 90° angle to the window which means that the surface can be illuminated by direct sunlight. From the measurement results presented in chapter 6 it was seen that putting solar cells in a 90° angle to the window was the better orientation for harvesting energy. Depending on the thickness of the frame that is attached to the window there might however be some cases when the long side of the magnet contact sensor is shaded, in which case the advantage is lost. Because of this fact and because the front side has a larger surface area, it was decided to put solar cells on the front side of the magnet contact sensor.

It was decided to go for organic solar cells since they are projected to be cheap and because of the recent improvements in efficiency, as discussed in chapter 3.3.3. An organic solar cell module is also a good fit for the product since they are thin and because a module with a custom shape can easily be manufactured. The effective area of the solar cell module ended up being 16 cm^2 as some margins were left to the edges of the surface of the magnet contact sensor (for a final product the margins can be reduced).

The number of cells in series in the organic solar cell module was selected with the bq25505 energy harvesting chip in mind. When the voltage of the supercapacitor is below approximately 1.7 V the bq25505 chip will work in cold-start mode. In this mode the chip will clamp the voltage across the solar cell module to 0.3 V. For the chip to be able to charge the supercapacitor at a good rate in the cold-start mode it is therefore important that the solar cell module can deliver a high current at 0.3 V. For this reason the solar cell module was manufactured with only a few cells in series such that the OCV was approximately 1.3 V.

It was noted that the efficiency of the boost converter which is part of the bq25505 chip is highly dependent on the voltage and current. To optimize the prototype further it would therefore be necessary to test different solar cell modules with different number of cells in series to find a balance between high efficiency and the ability to leave cold-start mode.

7.2.1 Energy harvestable in natural light

A rough estimation of the amount of energy that can be harvested per day for the different months of the year was made. The estimation was made by extrapolating values measured in May, as presented in chapter 6.2.1, using data from the Swedish Meteorological and Hydrological Institute (SMHI).

The extrapolation was based on the harvestable energy per area per day as measured in May for the case when the organic solar cell module was mounted at a 180° angle to the window (values from Table 8). It was first assumed that the measurements were made in June, since they were actually made in late May on the 24th, as to not overestimate the energy. The harvestable energy per area was calculated for each month by scaling the value for June with the ratio between global irradiance in June and for each month, as found in the data from SMHI (normal values of global irradiance for 1961-1990 in Lund, southern Sweden[12]).

The extrapolated values for harvestable energy per area were then multiplied by 16 cm^2 to get absolute values for the energy that can be harvested per day with the solar cell module used in the prototype. The results of this estimation can be seen in Figure 33. It should be noted that the extrapolation is based on the measurements made in May on a mostly cloud-free day, and that a more realistic estimation would instead have to be based on an average of cloud-free and cloudy days.

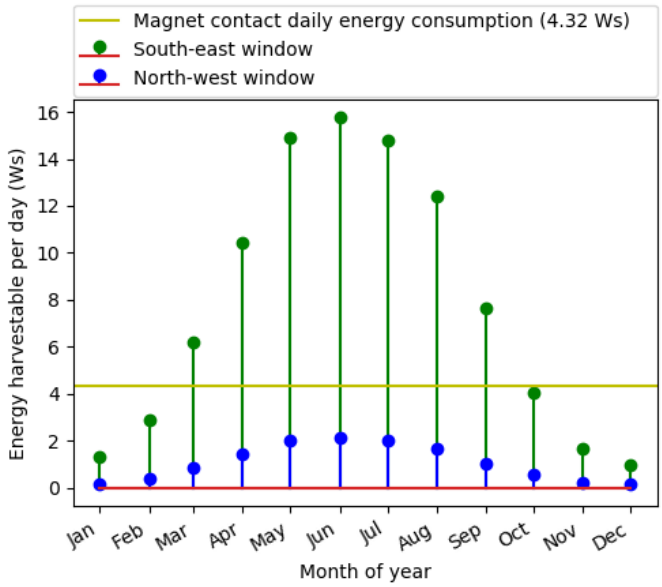

Figure 33: Estimated energy harvestable per day for each month of the year (16 cm^2 organic solar cell, 180° angle to window).

From Figure 33 it can be seen that the energy that can be harvested in north-west facing windows is not enough to supply the energy consumed by the magnet contact (4.32 Ws). For a south-east facing window the graph shows that there is an abundance of energy from March to September.

Appendix C shows the same energy estimations, made for all three solar cell types tested in chapter 6, assuming instead a solar cell module of 20 cm^2 corresponding to the full front side area of the magnet contact node.

[12] Based on monthly data for global irradiance in Lund from SMHI 2017-files (normal values for 1961-1990). Available at: https://data.smhi.se/met/climate/time_series/month/vov_pdf/, accessed 2018-04-26.

7.2.2 Energy harvestable in artificial light

An estimation of the amount of energy that can be harvested in the light from LED, CFL and halogen lamps was also made. The estimation was based on the measurement results for organic solar cells presented in chapter 6.3.1.

The estimation was made for a total of four different cases; two different levels of illuminance and two different values for the number of hours that the lamps are turned on per day. The two levels of illuminance were 100 and 250 lux and the number of hours were 6 and 12 hours. The levels for illuminance were selected as the two levels for which data had been collected in 6.3.1 which were closest to the level of illuminance recommended for general lightning in a living room (100-200 lux according to a guide by lamp retailer Beacon Lighting Commercial [62]). During winter time it was considered reasonable to have lamps turned on for 6 hours or more if you get home from work at 6 pm and go to sleep at 12 pm. Having the lamps turned on for 12 hours per day was included as an extreme case.

Table 15: Estimated energy harvestable in artificial light (16 cm^2 organic solar cell module, percent of magnet contact daily energy consumption shown in parenthesis).

Number of hours per day with lamps turned on (h)	Illuminance (lux)	Energy harvestable in light from LED lamp (Ws)	Energy harvestable in light from CFL lamp (Ws)	Energy harvestable in light from halogen lamp (Ws)
6	100	0.33 (7.6 %)	0.29 (6.7 %)	0.60 (13.8 %)
	250	0.98 (22.6 %)	0.86 (19.9 %)	1.56 (36.1 %)
12	100	0.66 (15.3 %)	0.58 (13.4 %)	1.20 (27.7 %)
	250	1.96 (45.3 %)	1.72 (39.8 %)	3.12 (72.2 %)

Appendix C shows the same energy estimations, made for all three solar cell types tested in chapter 6, assuming instead a solar cell module of 20 cm^2 corresponding to the full front side area of the magnet contact node.

7.3 ENERGY STORAGE

It was decided to have a rechargeable storage with enough energy capacity to power the magnet contact during the night. The choice fell on a supercapacitor because they were easily obtainable and because of their looser requirements for operating safely.

By taking into account the power consumption of the magnet contact and the maximum leakage current of a particular supercapacitor of 1 F it was found that it would be able to power the magnet contact for 10.7 hours in the worst-case scenario. The leakage current of the selected supercapacitor was stated to be at max 6 µA after 72 hours [46]. By assuming that this level of leakage occurs at for example 3 V, the leakage power can be estimated as $3\ V \cdot 6\ \mu A = 18\ \mu W$, which shows that the leakage can be quite large in comparison to the average power consumption of 50 µW for the magnet contact.

7.4 POWER ELECTRONICS

It was decided to use an energy harvesting chip since the functionality they provide is convenient for the application. The particular chip that was selected is the bq25505 from Texas Instruments. This chip was selected since it is well documented, can automatically switch to a backup battery and because it did not include a voltage regulator on the output (which the magnet contact already has on the input).

A 3 V lithium CR2025 coin cell battery was used as backup battery such that bq25505 connects it to the output node when the voltage of the supercapacitor drops too low. The coin cell battery was not seen as the ideal backup battery, but was selected for the prototype because it could easily fit into the plastic casing of the magnetic contact without a mechanical redesign. The limitations of the coin cell battery include the fact that the capacity is fairly low, which makes it possible that the battery would have to be replaced after a while. Another limitation is that the voltage will drop substantially when drawing high currents, which the magnet contact periodically does. To prevent the voltage drop two big capacitors of 1.5 mF each had to be incorporated in the design.

7.5 PCB DESIGN

A two layer PCB was designed in a CAD program, basing the schematic and layout on the recommendations found in the datasheet of the bq25505 and the bq25505 evaluation module. The resistors in the resistor divider networks where chosen such that the voltage of the supercapacitor stayed within the acceptable voltage range of the voltage regulator of the magnet contact circuit (the chosen interval was approximately 2.4 V to 3.8 V). When the voltage of the supercapacitor falls below 2.4 V the bq25505 will then automatically switch to using the backup battery.

A battery holder was included on the bottom side of the PCB to be able to conveniently connect the backup battery. Pads were put on the board such that wires could be soldered to make all the external connections (supercapacitor, solar cell module and magnet contact alarm circuit).

The board was designed to fit inside the plastic casing of the magnet contact sensor and the final dimensions ended up being approximately 33x19 mm. Pictures of the 3D model for the board can be seen in Figure 34 and Figure 35. The full schematic and PCB layout can be seen in appendix B.

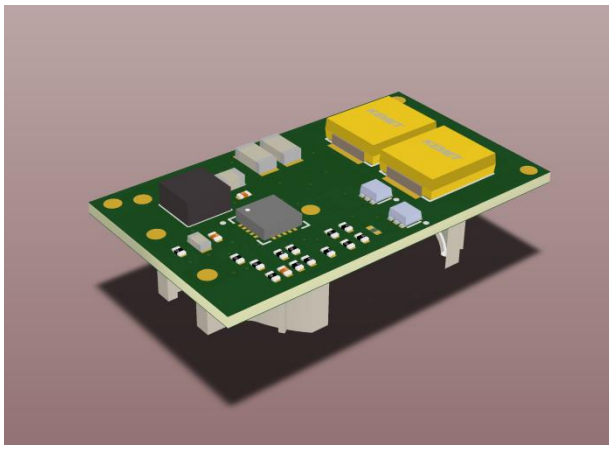

Figure 34: Top view of the PCB designed for the prototype.

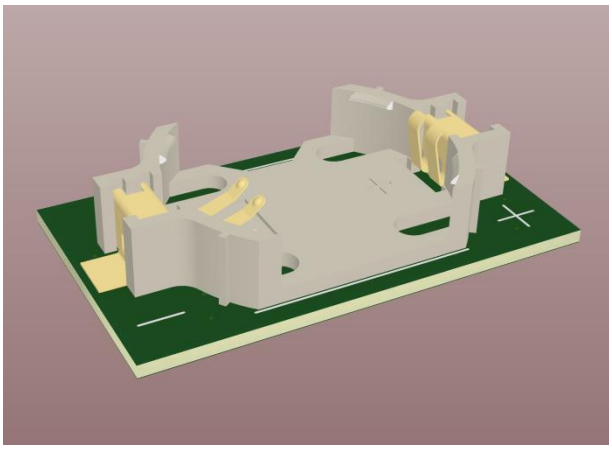

Figure 35: Bottom view of the PCB designed for the prototype.

7.6 ESTIMATION OF COST

An estimation of the cost of the energy harvesting solution was made and the results can be seen in Table 16. The cost of the solar cell module is based on the lowest price per area of amorphous silicon solar cells as found in chapter 3.3.5 since the price of the organic solar cell module was not available.

The cost of the backup battery, battery holder and the C5 and C6 capacitors is not included since these components are a result of the choice of primary battery. Because the particular battery was only selected based on the criteria of easily fitting inside the plastic casing of the magnet contact it was not relevant to include the cost.

The cost of the C3 and C4 capacitors are also not included in the table since they are not required in a final design. They were put on the board only to be able to test the functionality of the circuit without connecting the supercapacitor.

Table 16: Estimated cost of the energy harvesting solution built for the prototype.

	Designator(s)	Part description	Quantity	Price per unit (USD)
Solar cell module				1.76
	Connected to TP3 and TP4	Organic solar cell module, 16 cm^2	1	Not available
	Only used for estimating price of a solar cell module (not used in design)	Amorphous silicon solar cell module, 16 cm^2 (price per area for Panasonic AM-1816)[13]	-	1.76 / 1 ku
Energy harvesting circuit				3.49
	U1	TI bq25505	1	2.25 / 1 ku[14]
	L1	Coilcraft LPS4018-223	1	0.58 / 2 ku[15]
	Q1, Q2	Rohm US6J11TR 2 P-channel	2	0.22 / 3 ku[16]
	C1	Cap 4.7 µF 0805 X7R 10 V	1	0.039 / 3 ku[16]
	C9	Cap 4.7 µF 0603 X7R 6.3 V	1	0.021 / 4 ku[16]
	C2, C10	Cap 100 nF 0402 X5R 10 V	2	0.006 / 10 ku[16]
	C7	Cap 10 nF 0402 X7R	1	0.02 / 5 ku[16]
	R1-R13	Various resistors	13	~0.01 / 100 ku[16]
	C3, C4	Cap 47 µF 1206 X5R 6.3 V	2	Not included in cost
	C5, C6	Kemet T520H158M006ATE055 1.5 mF	2	Not included in cost
	J1	Keystone 1058TR coin cell battery holder	1	Not included in cost
Rechargeable storage				1.81
	Connected to TP1 and TP2	AVX Corporation SCMR18C105MRBA0 1 F	1	1.81 / 5 ku[16]
Backup battery				
	Placed in battery holder	3 V lithium coin cell CR2025	1	Not included in cost
TOTAL COST				**7.06**

It should be noted that the prices are valid for quantities of a few thousand units and that lower prices can usually be expected for larger quantities.

[13] This particular amorphous solar cell module was found to have the lowest price per area in the investigation described in chapter 3.3.5 (0.11 USD/cm^2).
[14] Price from Texas Instruments, http://www.ti.com/power-management/battery-management/energy-harvesting/products.html, accessed 2018-07-06.
[15] Price from Mouser, https://www.mouser.se/, accessed 2018-07-17.
[16] Price from DigiKey SE, https://www.digikey.se/, accessed 2018-07-17.

7.7 RESULTS

The PCB that had been designed was ordered from a manufacturer and the components were soldered onto it by hand. The functionality of the circuit was first tested in a lab environment to see that everything was working. It was verified both that the supercapacitor stayed under its maximum voltage limit and that the backup battery was being connected to the output node when the voltage of the supercapacitor dropped too low.

A first prototype was built by putting the supercapacitor and circuit board inside the plastic casing of the magnet contact. Inside the casing the circuit board was connected to both the magnet contact alarm circuit and to the supercapacitor. Since it was difficult to solder directly onto the electrodes of the solar cell module it was decided to drill hole through the electrodes and through the plastic casing of the magnet contact. Metal screws were then put through each hole, and next a washer and nut was put on each screw on the inside of the casing. Small wires were put between the casing and each washer before tightening the screws such that electrical contact was achieved between the solar cell module and the wires. The other end of each wire was then connected to the circuit board such that electrical contact was established between the board and the solar cell module.

The first prototype was tested, but it was quickly found that the supercapacitor was only being charged at a very slow rate and only for a few hours each day. This lead to the belief that the solar cell module was either damaged from the drilling or that the electrical contact between the circuit board and the solar cell module was bad. A second prototype was therefore built, this time leaving all components outside of the plastic casing of the alarm node (except for the alarm circuit itself). An identical solar cell module was then connected to the circuit board, this time using crocodile clips to connect to the electrodes.

The two prototypes were then tested simultaneously while positioned in the same window board and having the alarm nodes connected to the same alarm system. The alarm nodes were oriented such that the solar cells formed a 90° angle to the window, which is a more advantageous orientation compared to the real orientation in which it would be normally mounted. An Arduino Mega was then used to continuously log the electrical potential in the important nodes of the two prototypes (10 min intervals). It was confirmed that both magnet contact nodes transmitted the correct wireless data packets by monitoring the logs of the alarm panel to which they were connected. The results showed that the supercapacitor in the second prototype was charged at a much higher rate compared to the first prototype, confirming that the first prototype had a damaged solar cell module or a bad electrical connection. The test setup can be seen in Figure 36 and the measurement results can be seen in Figure 37.

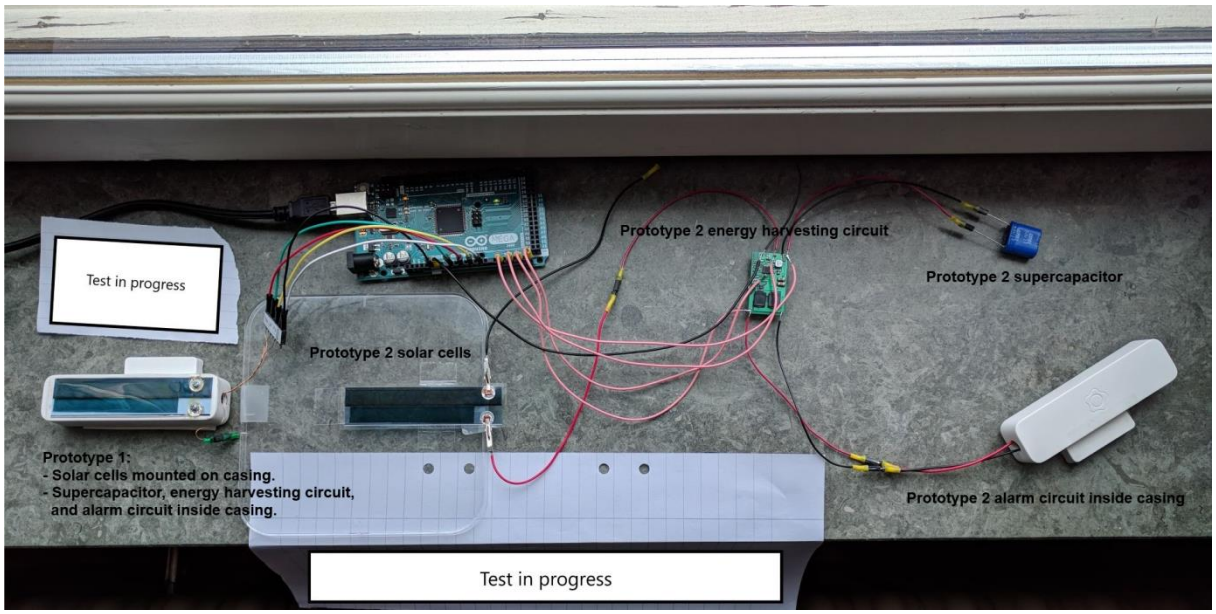

Figure 36: Test setup for the simultaneous measurements on the two prototypes.

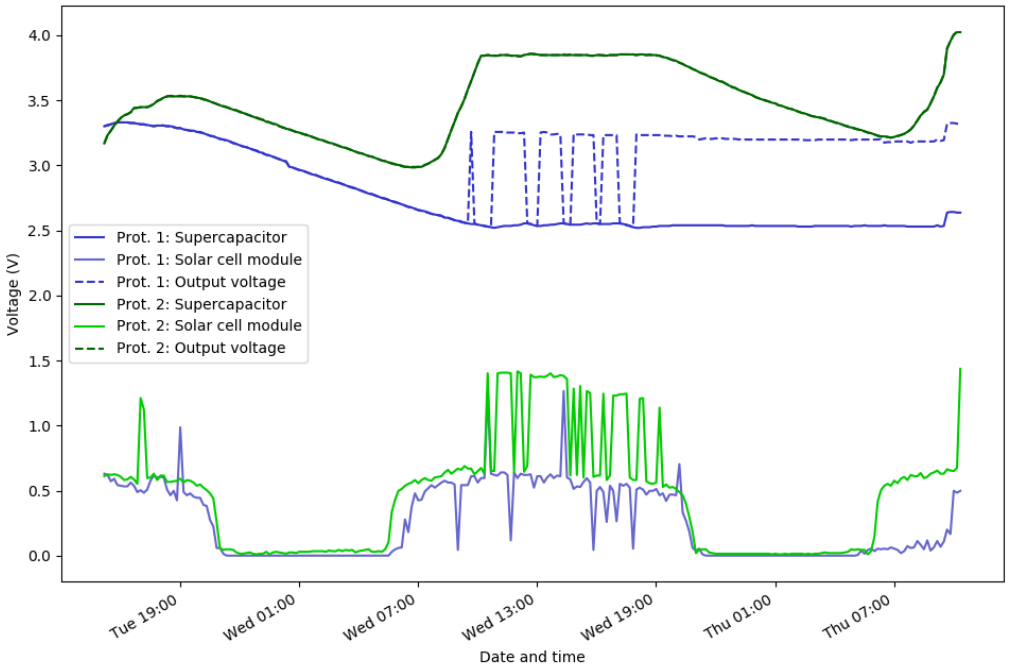

Figure 37: Result of the measurements made on the two prototypes (between the 14th and 16th of August 2018, south-east facing window, Malmö, Sweden).

It can be seen that prototype 2 is always using the supercapacitor as energy source when supplying the alarm node with power, since the dashed output voltage curve follows the supercapacitor curve. For prototype 1 it can be seen that the dashed output voltage curve does not always follow the supercapacitor curve, meaning that the output node of the PCB is connected to the 3 V lithium coin cell battery when the voltage of the supercapacitor is too low. For Wednesday it can be seen that the supercapacitor in prototype 2 stops being charged at a specific voltage, which corresponds well to the voltage limit which it was programmed to respect. On Thursday close to the end of the measurements, the curve of the supercapacitor voltage for prototype 2 shows that it exceeds 4 V, which is higher than the limit that was set. It can however be seen that there is a sudden jump in all

of the voltage curves, which lead to the belief that there was something wrong with the measurements. A multimeter was then used to confirm that 1) the voltage of the supercapacitor was in fact 3.68 V, which is under the voltage limit and 2) that the analog reference pin of the Arduino was at 4.57 V, whilst it was expected to be at 5 V (AREF pin). Recalculating the correct voltage values with the factor $\frac{4.57}{5}$ showed that the voltage of the supercapacitor was in fact below the maximum voltage limit. Since the Arduino Mega was powered over a USB cable, it was tested to instead power it with a wall power adapter and it was found that the analog reference pin would then rise to 5 V. It is believed that the anomaly at the end of the measurements was caused by a sudden change in voltage output by the USB socket.

The voltage over the solar cell modules can be seen to be approximately 0.6 V when the supercapacitors are being charged which corresponds to the programmed 50 % OCV fraction for the reference of the MPPT regulator. On Wednesday the solar cell module for prototype 2 went up to a higher voltage, a bit under 1.5 V, which corresponds to the OCV of the solar cell module. This voltage level was seen when prototype 2 stopped charging because the voltage of the supercapacitor had reached the limit.

From the results it can be seen that the supercapacitor is large enough to power the magnet contact throughout the night if it is fully charged.

8 DISCUSSION

This chapter discusses the results of the measurements and the information that was collected about the different questions that this thesis investigates.

8.1 SOLAR CELL TECHNOLOGIES

Crystalline silicon was found to be the solar cell type which dominates the market today. While this type of solar cell can harvest much more energy compared to e.g. amorphous silicon solar cells, their use in wireless alarm nodes may be less favored due to their higher cost. Amorphous silicon solar cells are more favorable in this aspect since they are cheaper and have proven use in smaller electronic products. They can possibly be easier to integrate mechanically because they can be made thinner and mechanically flexible. While the lifetime cannot compete with that of crystalline silicon solar cells, the lifetime of 15 years should be enough since the alarm system by then most likely has been replaced due to other factors such as outdated technology.

Organic and dye-sensitized solar cells which belong to the third generation solar cells are interesting contestants to the more established amorphous silicon solar cells. They show good potential for the use in smaller electronics products since they can be produced cheaply, because they are thin and flexible and because they work well in low light environments. Literature reports that they can sometimes harvest more power in indoor light conditions compared to amorphous silicon solar cells, such as in fluorescent light. This could however not be confirmed by the measurements described in chapter 6. The lifetime is reported to be much shorter compared to amorphous silicon solar cells and could possibly be a problem for the use in wireless alarm nodes. More data about the gradual loss of power capacity is required to deduce if the lifetime is a problem or if the capacity that is lost during the lifetime of the product is acceptable.

Another aspect which may become more important in the future is the use of low-E windows. Because low-E windows increase the energy efficiency of a house since heat does not escape as easily it reasonable that they will become more popular over time. Low-E windows attenuate the IR wavelengths and can thus reduce the benefit of using solar cells such as crystalline silicon solar cells which have low bandgaps.

A direct price comparison among different solar cells could not be made since there was a lack of publicly available price data for the new technologies. From the prices collected from DigiKey it was found that amorphous silicon solar cells were available from 0.11 USD/cm^2. It can be argued that solar cells in the third generation need to compete with this price considering that they generally still have lower efficiencies and lifetimes compared to amorphous silicon solar cells.

8.2 ENERGY STORAGE

Three different types of energy storage devices have been investigated in this report; capacitors, supercapacitors and batteries.

The energy capacity of normal capacitors is generally too low to store enough energy for supplying wireless alarm nodes with power for more than short periods of time. Depending on the physical constraints of the product it may not be possible to put in multiple capacitors to reach high energy capacities due to their low energy density. The main use for capacitors is as voltage stabilizers to prevent the voltage of batteries from dropping too low when there is a peak in load current.

The main advantages with supercapacitors are that they have higher energy densities compared to normal capacitors and that they can generally survive more charge and discharge cycles compared to batteries. A disadvantage with supercapacitors is that they have high leakage currents which can be of such order of magnitude that it is comparable to the power consumption of small wireless alarm nodes. If the power that can be harvested from the solar cells is scarce, the high leakage current can be very prominent, especially so if the supercapacitor is meant to store energy for longer periods of time.

If the goal with harvesting energy is to store enough energy to power alarm nodes over weeks or months it can be necessary to use batteries if physical space is scarce. The low leakage current compared to the leakage in supercapacitors is also favorable if the energy is stored for long periods. The operation of batteries usually needs more control compared to a supercapacitor to operate safely and to maintain a good lifetime. The lifetime of a battery is also usually shorter compared to a supercapacitor, and the design must consider how much the capacity will fade during the lifetime of the product.

Many batteries have fairly flat voltage characteristics whereas the voltage of capacitors varies widely with the state of charge. Since the voltage of batteries is more fixed it can be easier to design an electrical solution which works at a good efficiency compared to when the voltage is varying over a wide range. With clever design and matching between the MPP of the solar cells and the nominal voltage of the battery it might be possible to work close to the MPP without the use of an MPPT chip and thereby reduce the cost of the solution.

In chapter 4.2.4 it was found that the price of supercapacitors is generally higher compared to the price of batteries when talking about the price per capacity. For a more accurate price calculation for an individual application it would however be required to consider if the supercapacitor is never used below a certain voltage and if the battery is used with a DoD less than 100 %.

8.3 POWER ELECTRONICS

To extract maximum power from solar cells it generally a requirement to have a power converter that is controlled according to a MPPT scheme. The exception is if the solar cell is made to charge a battery with a flat voltage profile and a nominal voltage close to the MPP of the solar cell, in which case the same functionality is achieved through good design.

When working with energy storage devices it is required that the electrical solution keeps the storage within the correct voltage limits. For a capacitor the limit is a maximum voltage while batteries have both a maximum and a minimum limit. Special chips targeted for energy harvesting implement both MPPT and limit the voltage of the storage element. Some of these chips also include the functionality to switch to a backup battery at times when the voltage of the rechargeable storage is too low and some include a voltage regulator at the output. The disadvantage with these chips is that they come with a cost of 2-3 USD which can be a substantial amount of the total cost of the energy harvesting solution. When using an energy harvesting chip the designer should also consider how the efficiency of the power converters depends on the operating point of the solar cells.

Solar cells can also be used without MPPT by letting them freely charge a capacitor, although the power output from the solar cell will then vary widely depending on the state of charge of the capacitor. The advantage of such a solution is that it can be made very cheap and the disadvantage is that it will extract less power. To fully understand how the amount of power extracted compares to the power extracted for a system with MPPT it will be necessary to perform simulations or tests in

which the capacitance, power consumption of the load and how the incident light naturally varies must be accounted for.

8.4 MEASUREMENTS

The measurements have shown that the there is a large difference between the amount of energy that can harvested in window locations and at the inside of front doors and among the different types of solar cells. For the front door measurements it was found that the energy that could be harvested would cover 65 % of the daily energy consumption of the magnet contact at best.

The monocrystalline silicon module outperformed the other modules by far when it was placed in the south-east window at a 90° angle to the window. When placed at front door 1 the amorphous silicon module could compete with the crystalline silicon module, harvesting approximately the same amount of energy. This can possibly be explained by the fact that front door 1 never received direct sunlight and that the light that reached this location was mostly from reflection from walls. It can be the case that the material and paint of the walls reflect the visible light better compared to the IR waves, although this was not investigated deeper.

The organic solar cell module could harvest up to approximately half the amount of energy compared to the amorphous silicon module. Although no data for the efficiency of the investigated modules was available, if an assumption is made that the amorphous silicon module worked at 10 % that would put the organic solar cell module at approximately 5 %. The difference in performance between the two modules was bigger when they were placed such that they received direct sunlight. It should be noted that the particular amorphous silicon module that was tested has a thick glass substrate while the organic solar cell is a thin plastic film. The amorphous silicon solar cell is also available as a thin film, but wasn't obtainable from DigiKey and hence was not tested. From comparing the rated maximum power of amorphous silicon modules with glass substrates for outdoor applications and general purpose amorphous silicon modules in thin films, both from Panasonic, it was found that the glass substrate cells had a rated power per area that was approximately 25 % higher[17]. The difference indicates that a thin film version of the amorphous solar cell can harvest less energy than the glass substrate version, however this could not be deduced with certainty since there can be other differences between the versions that were compared. For a fair comparison between amorphous and organic solar cells it would however be required to get hold of a thin film amorphous solar cell.

The measurements have shown that window locations are interesting for harvesting energy for the magnet contact alarm node. Depending on the choice of solar cell, mounting angle and time of the year it can be expected to harvest a good amount of energy in relation to the energy consumption of the magnet contact alarm node which is often positioned in such locations. As is expected, it was found that there is a big difference between the amount of energy that can be harvested in a north-west facing window and in a south-east facing window. In Figure 33 it was seen that the energy harvestable by the prototype in the north-west window was never enough to fully sustain the magnet contact. This fact means that the product will need to have a large backup battery, which will be more utilized in the north-west window compared to the south-east window. The difference between windows appears to be eliminated on cloudy days on which most of the light is diffuse and

[17] Based on comparison of average rated output power per area of AM-5613, AM-5608 and AM-5605 to average rated output power per area of AT-7665, AT-7664 and AT-7666 for both "100 mW/cm^2" conditions and "SS-50k lux (Initial)" conditions. The values for the rated power of each product were found in the datasheet available at: https://media.digikey.com/pdf/Data%20Sheets/Sanyo%20Energy/Amorphous_Br.pdf (accessed 2018-08-27).

no direct sunlight is incident on the solar cells (as seen in chapter 6.2.3). The measurements also showed that much more energy can be harvested if the solar cell is mounted in a 90° angle to the window compared to if it is mounted at a 180° angle. For the case of the magnet contact alarm node it would therefore be beneficial if the mechanical casing of the product could be modified to allow the solar cells to face the optimal angle, which lies somewhere in between 0° and 90° between the solar cell and window.

In the end the measurements that were made in the home environment should only be used as rough estimates since they do not investigate the average weather conditions. For the prototype a year round extrapolation of the harvestable energy was made based on values measured on sunny days. For a better estimation it would be desirable to make measurements over longer periods of time, e.g. a full month, and then calculate the average harvestable energy per day. This value could then be extrapolated to all months of the year using the same method, but likely resulting in a more accurate prediction.

It must also be considered if the AREF pin of the Arduino might have experienced similar voltage drops as seen in chapter 7.7. By measuring the AREF voltage of the same setup used for the home environment measurements it was found that it was approximately 4.95 V. It can however not be concluded with certainty that the USB socket voltage didn't drop lower during the home environment measurements as the minimum acceptable voltage according to the USB 2.0 standards is 4.4 V [63]. If a worst-case scenario of 4.4 V is assumed it would mean that all measured currents and voltages would need to be multiplied with $\frac{4.4}{5} = 0.88$, which means that the calculated output power of the solar cells should be multiplied by $0.88^2 = 0.77$. This suggests that the energy harvested by the solar cells can be up to 23 % lower compared to what was presented in chapter 6.2.

The measurements that were made in artificial lights showed that the energy that can be harvested per day is fairly low if the solar cells are not placed very close to the light source. During winter time when there is not as many hours of daylight and artificial lighting is heavily relied on in the northern latitudes the artificial lighting does play a more important role compared to summer time. Basing the estimation of harvestable energy on artificial light is however not very reliable since there are no guarantees that an alarm node will be in the vicinity of a lamp and that the lamp is on. In settings such as industrial warehouses the artificial lighting is more predictable as compared to personal homes and one could possibly rely more on this type of light when estimating the amount of harvestable energy.

For the prototype it was shown that lamp light could supply between 6.7 % and 22.6 % of the daily energy consumption of the magnet contact for 6 h of light from a LED or CFL lamp with light levels typical for a living room. For 12 hours of light, the same values were between 13.4 % and 45.3 %, although it is believed that it is unrealistic to keep the lights on for such a long period of time. The same values for halogen lamps were significantly higher, reaching up to 36.1 % for 6 hours and 72.2 % for 12 hours, although this lamp type also consumes more energy and is probably not used as much. The levels shown are not enough to fully sustain the magnet contact alarm node, although it does help especially during winter time when there is less natural light.

8.5 PROTOTYPE

A prototype of a solar cell driven magnet contact alarm node was built and tested. The prototype was built to demonstrate the concept and to better understand the challenges. From the test that was performed it was found that the prototype seems to be working functionality wise, but will require further investigations such as measuring the efficiency of the circuit and assessing the light

conditions that are required for the supercapacitor to sustain its voltage level when the load is connected.

The choice of a coin cell battery as backup battery was made since the battery could easily be fitted into the product. The choice of this type of battery is however not optimal due to its low current capabilities and energy capacity. Tests must be carried out to find out how long a coin cell battery can sustain the device before it is depleted, and to assess if this is long enough to have the product survive its lifetime. The large capacitors of 1.5 mF each that were incorporated in the design because of the low current capabilities of the battery were electrolyte based capacitors. Such capacitors have a high current leakage which can further increase losses in the device. If large capacitors are still used in a future design another type of capacitor should be considered.

All components in the electrical solution must be selected to have as low losses as possible. Some possible component candidates of the prototype had to be declined due to having a footprint which made it hard to solder by hand. For a final design each component should be compared to alternatives with lower losses.

The PCB of the prototype takes up a considerable amount of space in the casing of the magnet contact alarm node. It is believed that the size can be reduced with a tighter PCB design, but that the solution will still take up a considerable amount of space in the product. This limits the type of backup battery which can be used if the current mechanical design should be conserved.

The cost of the prototype was found to be 7.06 USD by considering 16 cm^2 of amorphous solar cells instead of the organic solar cells (as no price data was available for the organic solar cells). This cost does not include the cost of the components related to the backup battery which is the C5 and C6 capacitors, the battery holder, the coin cell battery itself and does also not include the C3 and C4 capacitors which are not needed in a final design.

As a comparison, the two AAA batteries that are normally used to power the device are available from approximately 0.2 USD/unit for a quantity of 1000 units[18]. This suggests that using batteries is a cheaper option compared to harvesting energy with solar cells, although it must be remembered that the solution that was built for the prototype uses an energy harvesting chip and that it is possible to build cheaper solutions but with lower efficiencies (as described in chapter 5.3).

8.6 Prolonging battery life

An energy harvesting solution does not necessarily have to replace the primary batteries that are typically used to power the alarm nodes, but could instead be used as an addition to increase the battery life of the same batteries. By not including any rechargeable storage, except for very small capacitors to act as voltage stabilizers, the energy harvesting system can be made much cheaper. The solar cell module will then only harvest as much power as is consumed by the alarm node at every instant. When trying to estimate how much energy the solar cells will provide it is no longer possible to rely on the energy tables in chapter 6, since these are only valid under the assumption that the solar cells can always output maximum power. The electrical solution for prolonging battery life could look like the solution shown in chapter 5.3 (Figure 7). The backup battery, as shown in the schematic, would then be the primary batteries that are used to power the alarm nodes today. The primary batteries would then only be used when the solar cells cannot provide enough power, which effectively achieves the goal of prolonging battery life.

[18] Price from DigiKey SE, https://www.digikey.se/, accessed 2018-08-29.

9 CONCLUSIONS AND FUTURE WORK

This thesis has investigated how solar cells can be used to harvest energy for wireless alarm nodes. The different subsystems of an energy harvesting solution have been investigated and discussed with the application in mind. It can be concluded that there exist many ways to design such a system and that the choice of design is very dependent on how much the solution is allowed to cost.

The measurements of the amount of energy that can be harvested showed that there is a big difference between different solar cells, locations and orientations. For a south-east facing window you can fully power the magnet contact alarm node for a good part of the year. This is however not true for north-west facing windows and front doors. The same alarm product can therefore be expected to be working under very different conditions depending on where it is installed in the house. As a result, the batteries of some alarm nodes will need to be changed more often compared to others. The worst locations in which the alarm nodes are installed in a house will then decide how often a service to change batteries is needed. The potential cost savings from reducing the servicing frequency, which could be one of the major benefits of using solar cells, is therefore limited by this fact.

The prototype that was built demonstrated a particular solution for harvesting energy for the magnet contact alarm node. From the short evaluation that was made it could be concluded that the system is working functionality wise and that it can supply the alarm node with enough power on cloud free summer days in southern Sweden.

The following list contains suggestions of further studies that can be made on the subject of this thesis:

- To improve the estimation of the amount of energy that can be harvested in home environments it would be beneficial to make further measurements to increase the dataset. The measurements should be made over a longer period of time, continuously logging the MPP of the solar cells and in multiple houses. This would give more information about the average harvestable energy which could then be extrapolated for a more accurate year-round estimate compared to the one presented in this report.
- An energy harvesting solution which does not use MPPT should be built and benchmarked against a solution which does use MPPT (solutions without MPPT were discussed in chapter 5.3). This would show how the efficiency achieved by clever design and voltage matching compares to the efficiency achieved by using MPPT. The results should then be put in relation to the cost of the MPPT functionality, e.g. the cost of an energy harvesting chip like bq25505.
- The temperature dependence of the different solar cell technologies was briefly mentioned, but to fully understand how they behave it would have to be tested in a climate chamber. For organic and dye-sensitized solar cells it is extra important that this test should be made on the specific product of interest since there are a large number of different “blends” with different properties.

ACKNOWLEDGEMENTS

My thanks go to the people at Verisure Innovation who came up with the idea for the project and presented the opportunity to work on this thesis. Jonas Johannesson, who was my main contact at Verisure Innovation, was always available for discussing ideas or problems related to the thesis. His guidance was superb in every way and I am very thankful for his support and humoristic mood. I thank also his many colleagues in the hardware department who supported me with everything from PCB design to answering questions about their products.

I also want to thank Gunnar Lindstedt and Johan Björnstedt at the Division of Industrial Electrical Engineering and Automation, Faculty of Engineering, Lund University. Gunnar who was my supervisor provided excellent support and guided me through the process of writing this thesis. Johan had the role as examiner and showed great interest in the project.

Further thanks go to the solar cell manufacturer who provided the organic solar cells used for the measurements and for the prototype. They also provided many useful ideas and enthusiastically shared their experience in the field.

REFERENCES

[1] "Solar Cell Structure," [Online]. Available: https://www.pveducation.org/pvcdrom/solar-cell-structure. [Accessed 06 03 2018].

[2] "Light Generated Current," [Online]. Available: https://www.pveducation.org/pvcdrom/solar-cell-operation/light-generated-current. [Accessed 06 03 2018].

[3] "The photovoltaic effect," [Online]. Available: https://www.pveducation.org/pvcdrom/solar-cell-operation/the-photovoltaic-effect. [Accessed 06 03 2018].

[4] "Solar Cell Efficiency," [Online]. Available: https://www.pveducation.org/pvcdrom/solar-cell-operation/solar-cell-efficiency. [Accessed 24 04 2018].

[5] P. P. Kumavat, D. S. Dalal and P. Sonar, "An overview on basics of organic and dye sensitized solar cells, their mechanism and recent improvements," *Renewable & Sustainable Energy Reviews,* vol. 78, pp. 1262-1287, 2017.

[6] "Measurement of Solar Cell Efficiency," [Online]. Available: https://www.pveducation.org/pvcdrom/characterisation/measurement-of-solar-cell-efficiency. [Accessed 24 08 2018].

[7] "Effect of Light Intensity," [Online]. Available: https://www.pveducation.org/pvcdrom/solar-cell-operation/effect-of-light-intensity. [Accessed 24 04 2018].

[8] "Quantum Efficiency," [Online]. Available: https://www.pveducation.org/pvcdrom/solar-cell-operation/quantum-efficiency. [Accessed 24 04 2018].

[9] "Effect of Temperature," [Online]. Available: https://pveducation.org/pvcdrom/solar-cell-operation/effect-of-temperature. [Accessed 21 08 2018].

[10] P. A. Tiples and G. Mosca, Physics for Scientists and Engineers, New York: W.H. Freeman and Company, 2008, pp. 684-685, 1080.

[11] "Atmospheric Absorption & Transmission," [Online]. Available: http://gsp.humboldt.edu/olm_2016/Courses/GSP_216_Online/lesson2-1/atmosphere.html. [Accessed 26 03 2018].

[12] H. Bülow-Hübe, "Fönsterfysik och energitransport genom fönster," [Online]. Available: http://www.lth.se/fileadmin/energi_byggnadsdesign/images/Utbildning/ABK100/F8_PM_f_nsterfysik.pdf. [Accessed 26 03 2018].

[13] M. Alaküla, L. Gertmar and O. Samuelsson, Elenergiteknik, Lund: Divison of Industrial Electrical Engineering and Automation, Faculty of Engineering, Lund University, 2011, pp. 115, 117.

[14] X. Ma, S. Bader and B. Oelmann, "Characterization of Indoor Light Conditions by Light Source Classification," *IEEE Sensors Journal,* vol. 17, no. 12, pp. 3884-3891, 2017.

[15] "Fraunhofer ISE: Fraunhofer Photovoltaics Report, updated: 26 February 2018," 2018.

[16] M. A. Green, "Third generation photovoltaics: solar cells for 2020 and beyond," *Physica E: Low-dimensional Systems and Nanostructures,* vol. 14, no. 1-2, pp. 65-70, 2002.

[17] A. Kaminski-Cachopo, "Solar cells for energy harvesting," [Online]. Available: https://www.nereid-h2020.eu/system/files/files/workshops/DWS/slides/DWS_WP42-2016-10-19-02Kaminski_NEREID_public.pdf. [Accessed 03 05 2018].

[18] "Solar cells - the three generations," [Online]. Available: http://plasticphotovoltaics.org/lc/lc-solarcells/lc-introduction.html. [Accessed 25 08 2018].

[19] NREL, "Low Cost III-V Solar Cells," [Online]. Available: https://www.nrel.gov/pv/low-cost-iii-v-solar-cells.html. [Accessed 03 08 2018].

[20] "Types of thin film solar panels," EnergySage, 20 03 2018. [Online]. Available: https://www.energysage.com/solar/101/about-solar-panels/thin-film-solar-panels-amorphous-cadmium-telluride-and-cigs/. [Accessed 21 08 2018].

[21] D. H. Nguyen, "Toxic Chemical in Solar Panels," 30 04 2018. [Online]. Available: https://sciencing.com/toxic-chemicals-solar-panels-18393.html. [Accessed 21 08 2018].

[22] National Renewable Energy Laboratory, "Efficiency Chart | Photovoltaic Research (NREL)," [Online]. Available: https://www.nrel.gov/pv/. [Accessed 25 07 2018].

[23] "Oxford PV," [Online]. Available: https://www.oxfordpv.com. [Accessed 25 08 2018].

[24] "Saule Technologies," [Online]. Available: http://www.sauletech.com. [Accessed 25 08 2018].

[25] "Single Crystalline Silicon," [Online]. Available: https://www.pveducation.org/pvcdrom/manufacturing/single-crystalline-silicon. [Accessed 03 05 2018].

[26] "Multi Crystalline Silicon," [Online]. Available: https://www.pveducation.org/pvcdrom/manufacturing/multi-crystalline-silicon. [Accessed 03 05 2018].

[27] A. McEvoy, T. Markvart and L. Castañer, Practical Handbook of Photovoltaics: Fundamentals and Applications, Academic Press, 2012, pp. 86-87, 212, 216, 223, 233, 497-499, 535-536, 544, 548-549, 554, 560.

[28] K. Patel, "Solar panel efficiency and lifespan," 21 09 2016. [Online]. Available: https://www.solarenergyforus.com/solar-panel-efficiency-lifespan/. [Accessed 27 08 2018].

[29] "Amorphous Silicon," [Online]. Available: http://www.solar-facts-and-advice.com/amorphous-silicon.html. [Accessed 25 07 2018].

[30] N. Marinova, S. Valero and J. L. Delgado, "Organic and perovskite solar cells: Working principles, materials and interfaces," *Journal of Colloid And Interface Science,* vol. 488, pp. 373-389, 2017.

[31] Y. Aoki, "Photovoltaic performance of Organic Photovoltaics for indoor energy harvester," *Organic Electronics,* vol. 48, pp. 194-197, 2017.

[32] K. Ghaffarzadeh, "Organic photovoltaics or dye sensitised solar cells - which will win?," 14 08 2012. [Online]. Available: https://www.idtechex.com/research/articles/organic-photovoltaics-or-dye-sensitised-solar-cells-which-will-win-00004647.asp. [Accessed 22 08 2018].

[33] N. Bristow and J. Kettle, "Outdoor performance of organic photovoltaics: Diurnal analysis, dependence on temperature, irradiance and degradation," *Journal of Renewable & Sustainable Energy,* vol. 7, no. 1, pp. 1-12, 2015.

[34] infinityPV, "Organic Solar Cells," [Online]. Available: https://solarenergyforus.com/solar-panel-efficiency-lifespan/. [Accessed 27 08 2018].

[35] N. Tanabe, "Fujikura: Dye-Sensitized Solar Cell for Energy Harvesting," 2013. [Online]. Available: http://www.fujikura.co.jp/eng/rd/gihou/backnumber/pages/__icsFiles/afieldfile/2013/05/23/42e_30.pdf. [Accessed 22 08 2018].

[36] "Dye sensitized solar cell," Fujikura, [Online]. Available: https://www.fujikura.co.uk/products/energy-and-environment/dye-sensitized-solar-cell/. [Accessed 22 08 2018].

[37] "Organic sensitizing dyes," Dyenamo, [Online]. Available: https://www.dyenamo.se/dyenamo_dyes.php. [Accessed 27 08 2018].

[38] "Customized Solar Cells," GCell, [Online]. Available: https://www.gcell.com/gcell-products/custom-solar-cell. [Accessed 27 08 2018].

[39] "Energy Storage Technologies," CAP-XX, [Online]. Available: https://www.cap-xx.com/resource/energy-storage-technologies/. [Accessed 12 07 2018].

[40] A. R. Hambley, Electrical Engineering: Principles and Applications (6th edition), Pearson Education Limited, 2013, pp. 143, 148, 154.

[41] A. Yu, V. Chabot and J. Zhang, Electrochemical Supercapacitors for Energy Storage and Delivery, Boca Raton: Taylor & Francis, 2013, pp. 6-7, 9, 11, 99.

[42] "No, a supercapacitor is not a capacitor," [Online]. Available: https://www.supercaptech.com/no-supercapacitor-is-not-a-capacitor. [Accessed 18 04 2018].

[43] H. Berg, Batteries for Electric Vehicles: materials and electrochemistry, Cambridge University Press, 2015, pp. 7-10, 62-66.

[44] M. Hassanalieragh, T. Soyata, A. Nadeau and G. Sharma, "Solar-supercapacitor harvesting system design for energy-aware applications," in *IEEE International System-on-chip Conference (SOCC)*, Las Vegas, 2014.

[45] O. Bohlen, J. Kowal and D. U. Sauer, "Ageing behaviour of electrochemical double layer capacitors. Part I. Experimental study and ageing model," *Journal of Power Sources,* vol. 172, no. 1, pp. 468-475, 2007.

[46] AVX, "SCM Series: Series-Connected SuperCapacitor Modules," [Online]. Available: http://datasheets.avx.com/AVX-SCM.pdf. [Accessed 20 07 2018].

[47] "BU-302: Series and Parallel Battery Configurations," 16 04 2018. [Online]. Available: http://batteryuniversity.com/learn/article/serial_and_parallel_battery_configurations. [Accessed 17 04 2018].

[48] "How does a supercapacitor work?," Battery University, [Online]. Available: http://batteryuniversity.com/learn/article/whats_the_role_of_the_supercapacitor. [Accessed 19 07 2018].

[49] "Battery VS Supercapacitor," SupercapTech.com, 21 05 2016. [Online]. Available: https://www.supercaptech.com/battery-vs-supercapacitor. [Accessed 19 07 2018].

[50] A. E. Ostfeld, "Printed and Flexible Systems for Solar Energy Harvesting," University of California, Berkeley, 2016.

[51] "BU-802b: What does Elevated Self-Discharge Do?," 04 04 2017. [Online]. Available: https://batteryuniversity.com/learn/article/elevating_self_discharge. [Accessed 21 08 2018].

[52] "BU-808c: Coulombic and Energy Efficiency with the Battery," 25 10 2017. [Online]. Available: http://batteryuniversity.com/learn/article/bu_808c_coulombic_and_energy_efficiency_with_the_battery. [Accessed 12 07 2018].

[53] H. Ibrahim, A. Ilinca and J. Perron, "Energy storage systems - Characteristics and comparisons," *Renewable and Sustainable Energy Reviews,* vol. 12, pp. 1221-1250, 2008.

[54] V. Musolini and E. Tironi, "A Comparison of Supercapacitor and High-Power Lithium Batteries," in *Electrical Systems for Aircraft, Railway and Ship Propulsion (ESARS)*, Bologna, 2010.

[55] S. Bush, "Tiny energy storage cell for IoT nodes lasts for years," 14 09 2016. [Online]. Available: https://www.electronicsweekly.com/news/products/power-supplies/tiny-energy-storage-cell-iot-nodes-lasts-years-2016-09/. [Accessed 21 08 2018].

[56] W. K. Ko, W. Xinhui, S. Dasgupta, W. J. Wong, R. Kumar and S. Panda, "Efficient solar energy harvester for wireless sensor nodes," in *IEEE International Conference on Communication Systems*, Singapore, 2010.

[57] J. Hernandez II, "How to implement maximum power point tracking for solar charging," Texas Instruments, [Online]. Available: https://training.ti.com/how-implement-maximum-power-point-tracking-solar-charging. [Accessed 12 04 2018].

[58] "bq25504 Ultra Low-Power Boost Converter With Battery Management for Energy," [Online]. Available: http://www.ti.com/lit/ds/symlink/bq25504.pdf. [Accessed 12 04 2018].

[59] "Energy Harvesting & Solar Charging," Texas Instruments, [Online]. Available: http://www.ti.com/power-management/battery-management/energy-harvesting/overview.html. [Accessed 12 04 2018].

[60] "bq25505 Ultra Low-Power Boost Charger With Battery Management and Autonomous," [Online]. Available: http://www.ti.com/lit/ds/symlink/bq25505.pdf. [Accessed 12 04 2018].

[61] "bq25570 Nano Power Boost Charger and Buck Converter," [Online]. Available:

http://www.ti.com/lit/ds/symlink/bq25570.pdf. [Accessed 12 04 2018].

[62] Beacon Lighting Commercial, "Lux levels guide: Domestic applications," 22 07 2014. [Online]. Available: https://www.beaconlightingtradeclub.com.au/media/Assets/LUX_Levels_Chart.pdf. [Accessed 29 08 2018].

[63] "USB 2.0 Specification," 27 04 2000. [Online]. Available: http://www.usb.org/developers/docs/usb20_docs/. [Accessed 05 09 2018].

APPENDIX A: PORTABLE SETUP FOR MEASURING I-V CURVES

A portable measurement unit which can measure the I-V curve of a solar cell was built using an Arduino Uno and an analog control circuit. The Arduino controls the amount of current from the solar cells by controlling the gate source voltage of a MOSFET transistor with the help of an OP-amp and a digital to analog converter (DAC). By ramping the current from the solar cell while also measuring the voltage and current it is possible to measure the I-V curve. The Arduino can transfer the measured values live to a PC for later analysis e.g. for finding the MPP.

The measurement setup is based on the measurement setup available at http://maecourses.ucsd.edu/callafon/labcourse/handouts/PV_Introduction_System.pdf, with the exception that here an Arduino is used to take the readings and also that some amplifier circuits were not used. A schematic of the measurement setup can be seen in Figure 38.

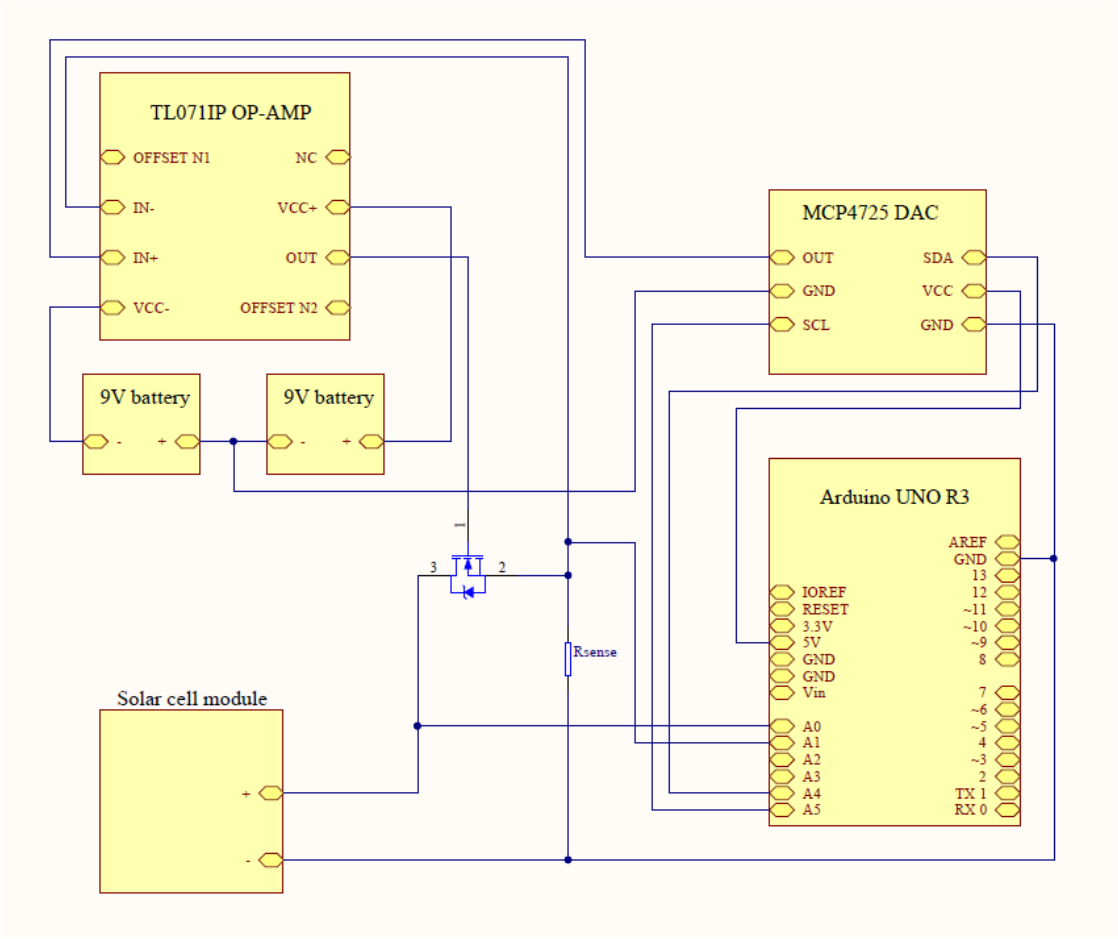

Figure 38: Schematic of the portable measurement setup for measuring I-V curves.

The resolution of voltage measurements is 4.9 mV, while the resolution of the current measurements depends on the resistance of the current sense resistor. The absolute accuracy of the ADC in the Arduino is ± 2 LSB, where LSB is the resolution previously mentioned[19].

[19] Accuracy stated in datasheet of ATmega328/P, http://ww1.microchip.com/downloads/en/DeviceDoc/ATmega328_P%20AVR%20MCU%20with%20picoPower%20Technology%20Data%20Sheet%2040001984A.pdf, accessed 2018-09-05.

Different current sense resistors where used depending on the light conditions. When measurements are done in a well-lit area, such as in a window, a small resistor must be used to not limit the portion of the I-V curve that can be captured. In darker areas a larger resistor could be used to increase the resolution of the measurements. An example of an I-V curve captured for a monocrystalline solar cell is shown in Figure 39.

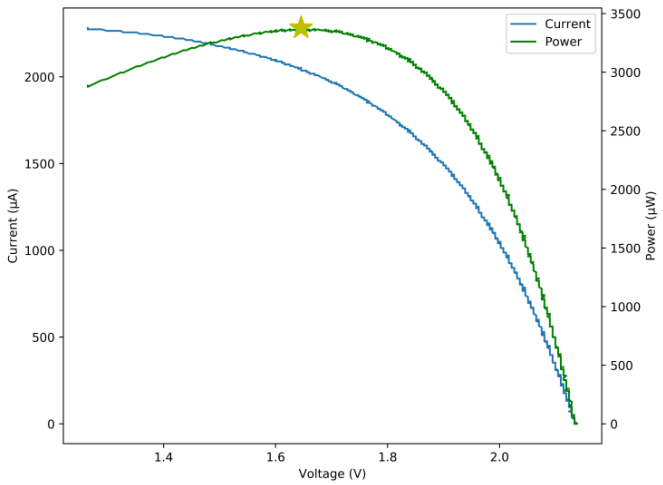

Figure 39: Example of an I-V curve captured by the Arduino based measurement setup.

APPENDIX B: SCHEMATIC AND LAYOUT OF THE PROTOTYPE BOARD

The schematic of the prototype board is shown in Figure 40 and the layout of the board is shown in Figure 41.

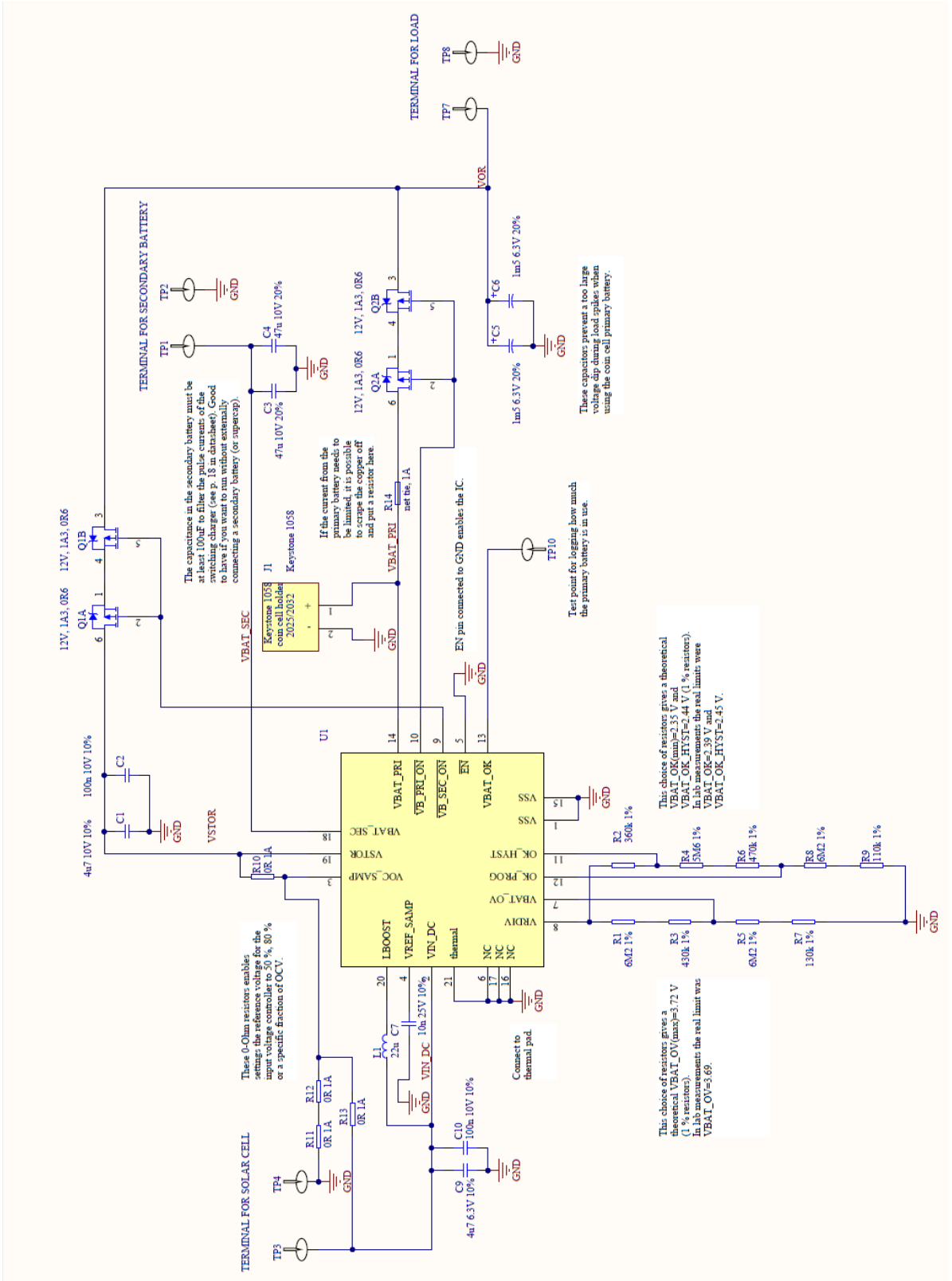

Figure 40: Electrical schematic of the prototype board.

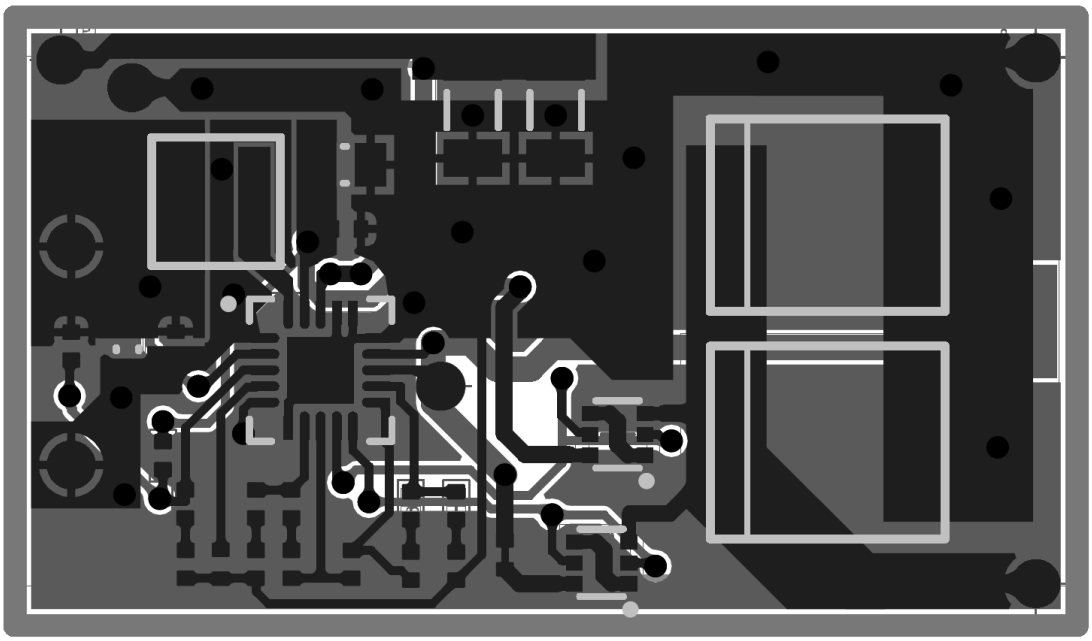

Figure 41: Layout of the prototype board.

APPENDIX C: ENERGY HARVESTABLE FOR MAGNET CONTACT

This appendix shows the results of estimating the energy that can be harvested by a 20 cm^2 solar cell module. The estimations are made for the three different types of solar cells that were tested in the measurements described in chapter 6. The results show the energy that can be harvested in natural light at windows and the energy that can be harvested in artificial light in a living room. For the estimations for windows it is assumed that the solar cell module is mounted with a 180° angle to the window. The estimations were made using the same procedures as described in chapter 7.2.1 and chapter 7.2.2.

Organic solar cell module (20 cm^2):

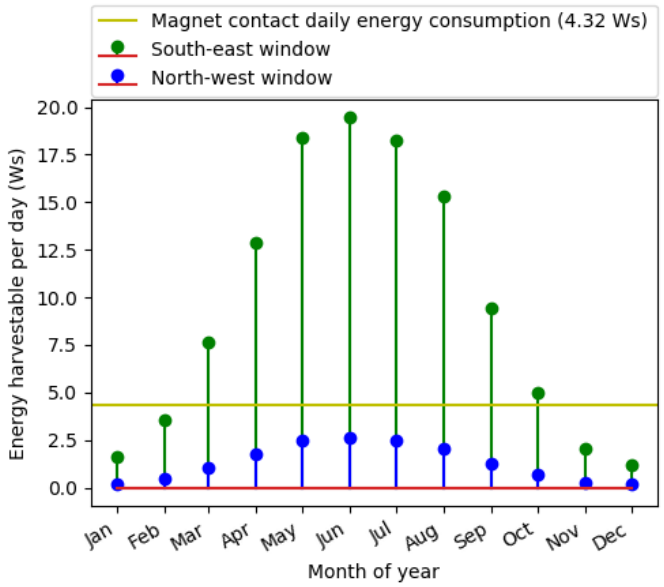

Figure 42: Estimated energy harvestable per day for each month of the year (20 cm^2 organic solar cell, 180° angle to window).

Table 17: Estimated energy harvestable in artificial light (20 cm^2 organic solar cell module, percent of magnet contact daily energy consumption shown in parenthesis).

Number of hours per day with lamps turned on (h)	Illuminance (lux)	Energy harvestable in light from LED lamp (Ws)	Energy harvestable in light from CFL lamp (Ws)	Energy harvestable in light from halogen lamp (Ws)
6	100	0.41 (9.6 %)	0.36 (8.4 %)	0.75 (17.3 %)
	250	1.22 (28.3 %)	1.08 (24.9 %)	1.95 (45.1 %)
12	100	0.83 (19.1 %)	0.73 (16.8 %)	1.50 (34.6 %)
	250	2.45 (56.6 %)	2.15 (49.8 %)	3.90 (90.3 %)

Amorphous silicon solar cell module (20 cm^2):

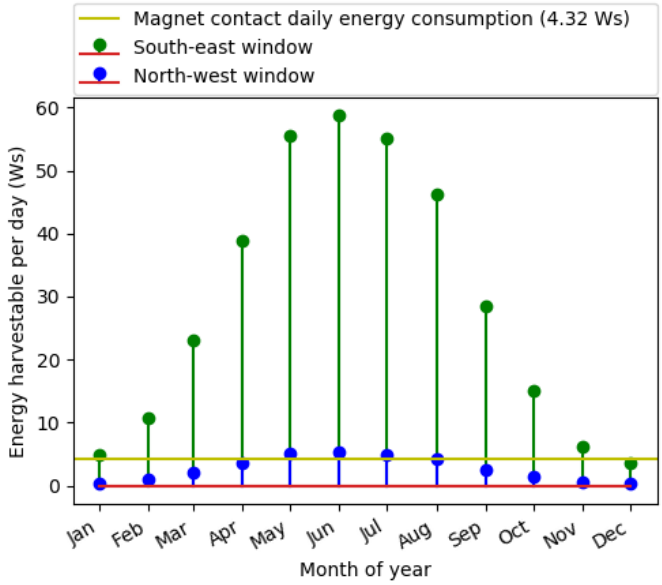

Figure 43: Estimated energy harvestable per day for each month of the year (20 cm^2 amorphous silicon solar cell, 180° angle to window).

Table 18: Estimated energy harvestable in artificial light (20 cm^2 amorphous silicon solar cell module, percent of magnet contact daily energy consumption shown in parenthesis).

Number of hours per day with lamps turned on (h)	Illuminance (lux)	Energy harvestable in light from LED lamp (Ws)	Energy harvestable in light from CFL lamp (Ws)	Energy harvestable in light from halogen lamp (Ws)
6	100	1.01 (23.4 %)	0.90 (20.8 %)	1.35 (31.2 %)
	250	2.53 (58.5 %)	2.34 (54.2 %)	3.18 (73.5 %)
12	100	2.02 (46.8 %)	1.80 (41.7 %)	2.69 (62.3 %)
	250	5.06 (117.0 %)	4.68 (108.3 %)	6.35 (147.0 %)

Monocrystalline silicon solar cell module (20 cm^2):

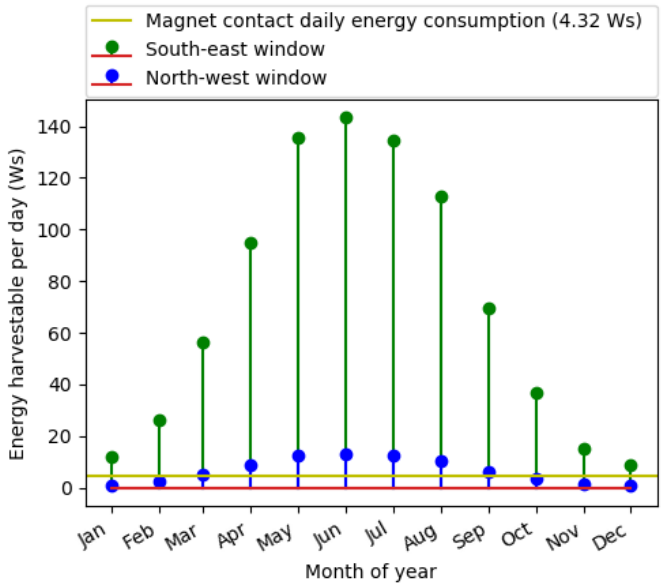

Figure 44: Estimated energy harvestable per day for each month of the year (20 cm^2 monocrystalline silicon solar cell, 180° angle to window).

Table 19: Estimated energy harvestable in artificial light (20 cm^2 monocrystalline silicon solar cell module, percent of magnet contact daily energy consumption shown in parenthesis).

Number of hours per day with lamps turned on (h)	Illuminance (lux)	Energy harvestable in light from LED lamp (Ws)	Energy harvestable in light from CFL lamp (Ws)	Energy harvestable in light from halogen lamp (Ws)
6	100	0.27 (6.4 %)	0.22 (5.1 %)	7.11 (164.6 %)
	250	1.10 (25.4 %)	0.91 (21.0 %)	19.97 (462.2 %)
12	100	0.55 (12.7 %)	0.44 (10.2 %)	14.22 (329.2 %)
	250	2.20 (50.8 %)	1.81 (41.9 %)	39.94 (924.4 %)